Simulation of the CDMSlite Detector's Response to Electron Recoil and Comparison to Experimental Data

PhD Defense, 2/9/2026

Lei Zheng

Outline

- **Introduction**
  - Evidence for Dark Matter and the WIMP Hypothesis
  - Overview of the SuperCDMS Soudan Experiment and the CDMSlite Detector
  - Thesis Goals
- **CDMSlite Detector Physics**
  - Electron Recoil Interactions
  - Detector’s Response and Output
- **CDMSlite Experimental Data for this work**
- **SuperCDMS Simulation and CDMSlite Simulation Samples**
- **Data Analysis**
  - Collection Efficiency
  - Energy Collection over Position and Time
  - Simulation-based Analysis Methods using Pulse Shape Characteristics (Rejecting Poorly-Measured Events, Estimating Interaction Positions, Calibrating Real Pulses)
  - Comparison of Pulse Shapes between Simulated and Real Experiment Data
- **Future Work and Conclusions**

Evidence for Dark Matter's Existence

Astronomical observations are significantly different from the expectations based on visible matter only, indicating there exists a large amount of invisible matter, which has been named '**Dark Matter**'. Here are two example pieces of evidence:

- **Galaxy Rotation Curve**
  Stars in a galaxy rotate around its center. The velocity is a function of the distance from the center.
  - Expected: The rotation velocity decreases at large R when considering visible matter only
  - Observed: Keeps increasing

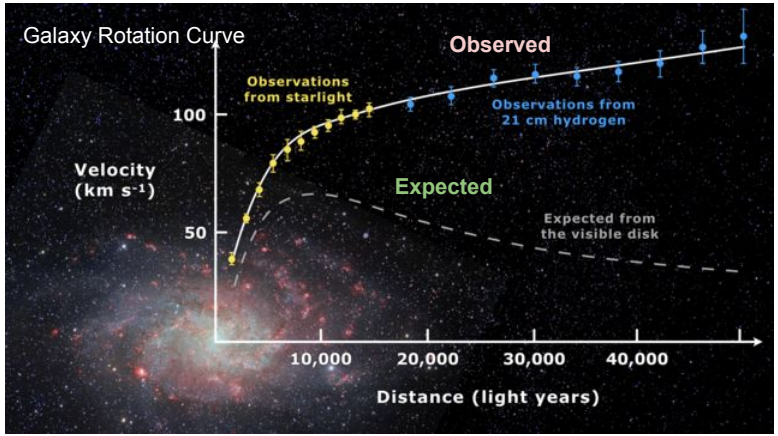

- **Einstein Ring (Gravitational Lensing)**
  The path of light from a far galaxy is bent by the gravity field of a near galaxy along the way. When these two galaxies and the Earth are on a straight line, the bent light forms a circular pattern (Einstein Ring).
  - Expected: A small ring due to the visible matter only
  - Observed: Much larger

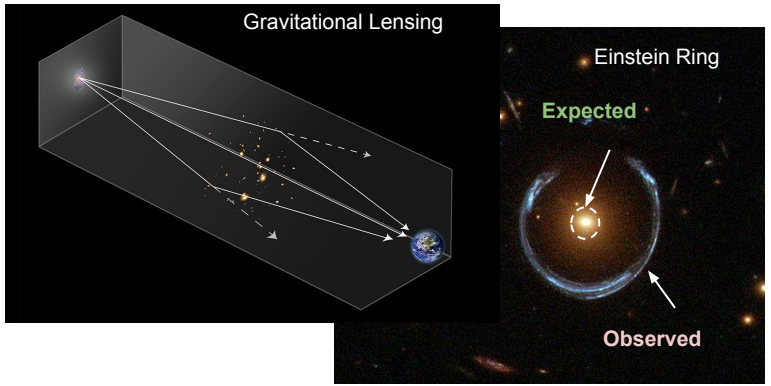

Evidence Indicating Dark Matter's Particle Properties and the WIMP Hypothesis

Further observation indicates that dark matter might be particles but doesn't interact electromagnetically. The Weakly Interacting Massive Particles (WIMP) hypothesis could explain the observations

- **Bullet Cluster**

  Two galaxy clusters colliding with each other
  - From X-ray observation (heat map of blue, red and yellow)
    Ordinary matter interacts and slows down
  - From gravitational lensing observation (green contours)
    Most of the mass passed through with little interaction

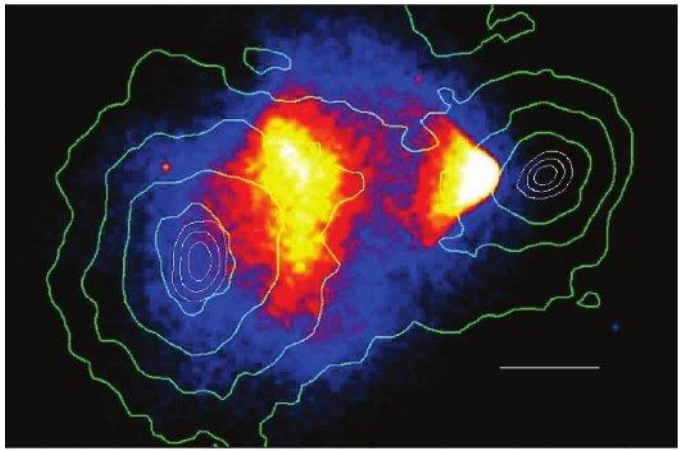

- **WIMP Hypothesis and Direct Detection**
  - Dark matter consists of electrically neutral particles that interact primarily via gravity and the weak nuclear force
  - A WIMP interacts weakly with the nucleus of a normal atom and transfers a small amount of energy, which allows **Direct Detection** methods to search for it

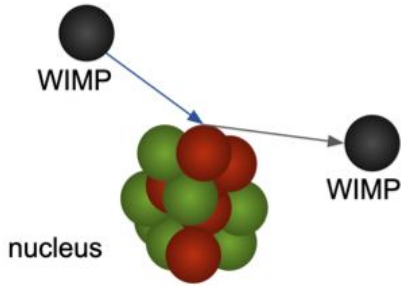

Overview of SuperCDMS Soudan Experiment and its CDMSlite Mode

SuperCDMS (Super Cryogenic Dark Matter Search) Soudan Experiments search for dark matter using direct detection methods, operated in the deep underground Soudan laboratory in Minnesota from 2011 to 2015

- Uses 15 germanium detectors to measure low energy from potential dark matter interactions (more details about the detector on the next page)

CDMSlite (Super**CDMS** **l**ow **i**onization **t**hreshold* **e**xperiment) is one of the SuperCDMS data-taking modes and aims to detect interactions from low-mass WIMPs, using a single detector (1114, CDMSlite detector)

- Targeting WIMP masses: 0.3 - 10 GeV/c^2
  Predicted energy deposits: <10 keV
- CDMSlite employs a high voltage (~70 V) across the detector to enable the measurement of such energy deposits by generating a lot of extra phonons (will describe more details later)

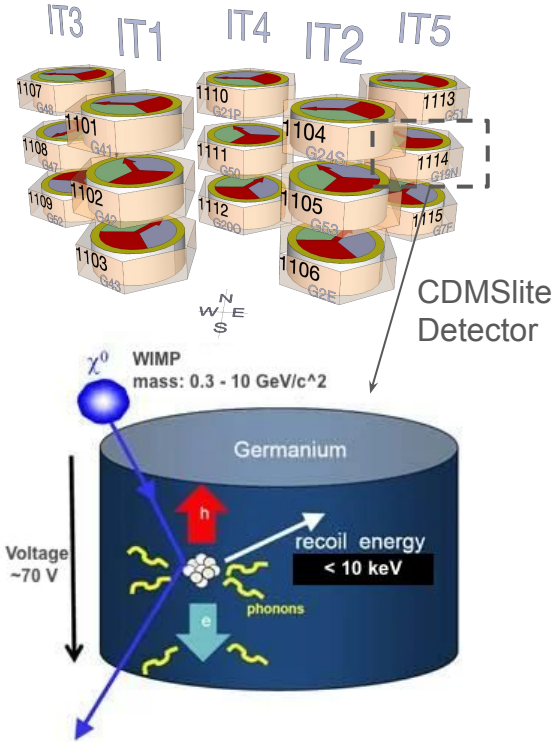

* threshold: the detector signal is only read out when the amount of energy is above a certain value

Main Components of the CDMSlite Detector

- **A germanium crystal**
  - Roughly cylindrical size: ~75 mm diameter, ~25 mm height (there are flats along the crystal edge)
  - Mass: ~600 g
- **Superconducting phonon sensors (QET*)**
  - Collect phonons for energy measurement
  - 400+ sensor units connected in series, forming a channel
  - Four channels
    - PA (the outer channel, ring-shape)
    - PB/PC/PD (the inner channels, fan-shape, symmetric)
- Electrodes (i.e. charge sensors)
  - Provide the voltage bias across the detector
- Copper housing
  - Grounded (0 V)
  - Provide pins for signal readout

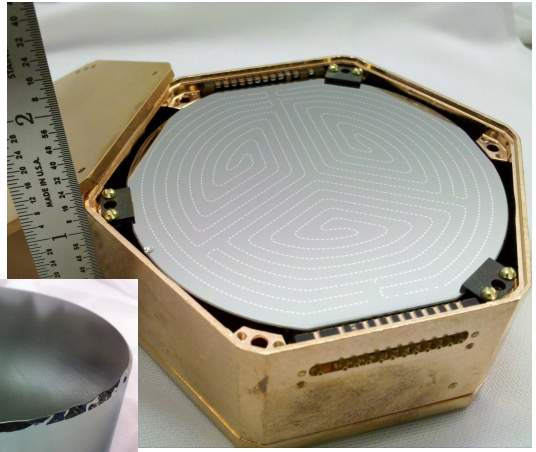

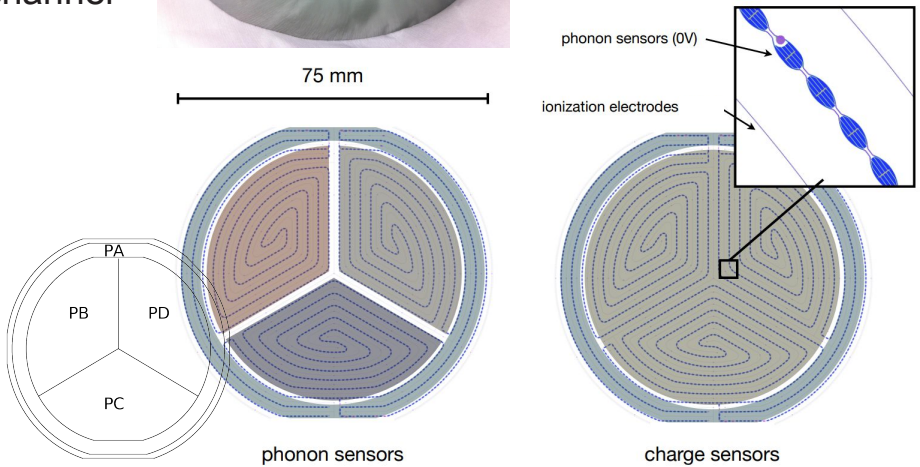

* QET: Quasiparticle Trap Assisted Electrothermal Feedback Transition Edge Sensor. A detailed description of how it works is given on Slide 17.

Overview of SuperCDMS Experiment Apparatus at Soudan Lab

For the detector operation, the **SuperCDMS** experiment apparatus provides a low-background (by multiple layers of lead, polyethylene, and veto system) and low-temperature environment, in addition to the cosmic-ray shielding from the overlying rock above the Soudan Lab

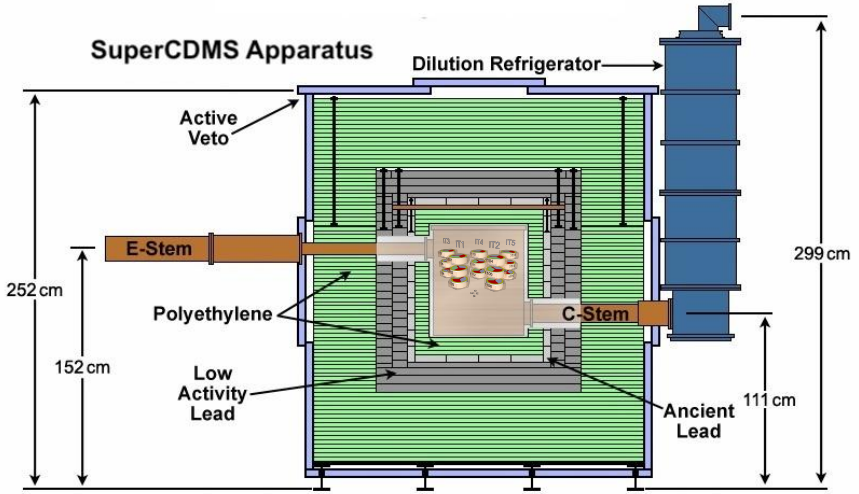

- The refrigerator and the cryogenic pipe (C-stem) provide the low-temperature (~ 50 mK) for the operation of detectors
- The electronics pipe (E-Stem) provide the electronics to read out detector signals
- Either C-stem or E-stem provides space for placing a neutron source (Cf-252) to produce Ge-71 for use in energy calibration

Motivation for this Work

- CDMSlite shows no evidence for dark matter as found
- All we get from the experiment are electronics signal pulses out of the sensors, from which physical information is inferred
- Previous CDMSlite analyses used a number of simplifying assumptions, which perhaps limited both the sensitivity and robustness of their results (e.g. energy measurement)
- To help maximize the sensitivity of the upcoming SNOLAB upgrade data taking, we need to better understand how an interaction produces the pulses so we can work backwards effectively
- Simulation can model the sophisticated microphysics processes underlying the detector's response to interactions, including the Ge crystal and phonon sensors (QETs), and produce the data with the same format as the real experimental data

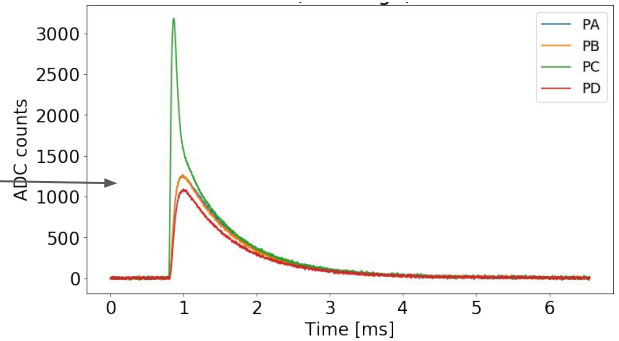

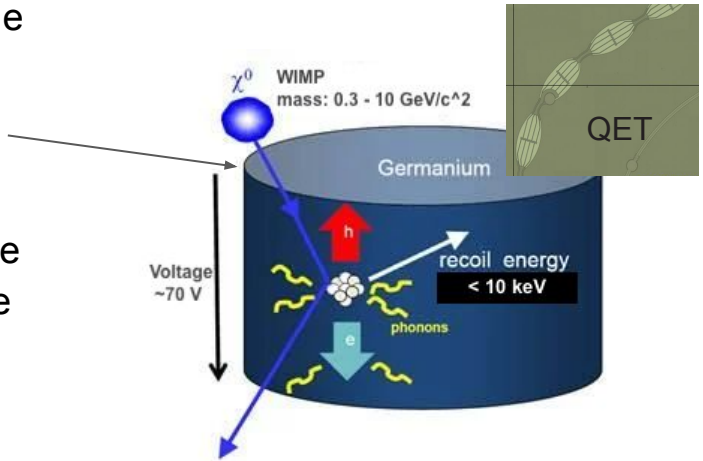

Goals of this Thesis

- To deepen our understanding of the detector's response to interactions via simulation and comparison to real experimental data, and further to advance the interpretation of real data

Questions we want to answer

- Can we reproduce the expected energy inside the detector in our simulation as well as the dominant mismeasurement causes?
- Are the previous models to describe the macroscopic output from billions of microphysical interactions well-justified? Can they be made better?
- Are the previous assumptions about the correlation between interaction positions and its signal pulses justified?
- Does the simulation suggest new methods to improve analysis (e.g. rejecting poorly-measured methods, estimating interaction positions, calibrating pulse scalings)?
- How well does the current version of the simulation reproduce what we see in the real data?

In the rest of the talk we will describe what we know about the related physics, the methods to answer these questions and present our results

Outline

- **Introduction**
  - Evidence for Dark Matter and the WIMP Hypothesis
  - Overview of the SuperCDMS Soudan Experiment and the CDMSlite Detector
  - Thesis Goals
- **CDMSlite Detector Physics**
  - Electron Recoil Interactions
  - Detector's Response and Output
- **CDMSlite Experimental Data for this work**
- **SuperCDMS Simulation and CDMSlite Simulation Samples**
- **Data Analysis**
  - Collection Efficiency
  - Energy Collection over Position and Time
  - Simulation-based Analysis Methods using Pulse Shape Characteristics (Rejecting Poorly-Measured Events, Estimating Interaction Positions, Calibrating Real Pulses)
  - Comparison of Pulse Shapes between Simulated and Real Experiment Data
- **Future Work and Conclusions**

Electron Recoil Interactions

Two types of interactions are expected to occur inside the CDMSlite detector:

- **Electron Recoil (ER)**
  - Interactions/scattering from the atomic electrons
  - Caused by photons and electrons
- Nuclear Recoil (NR)
  - Interactions/scattering from the atomic nucleus
  - Caused by WIMPs and neutrons

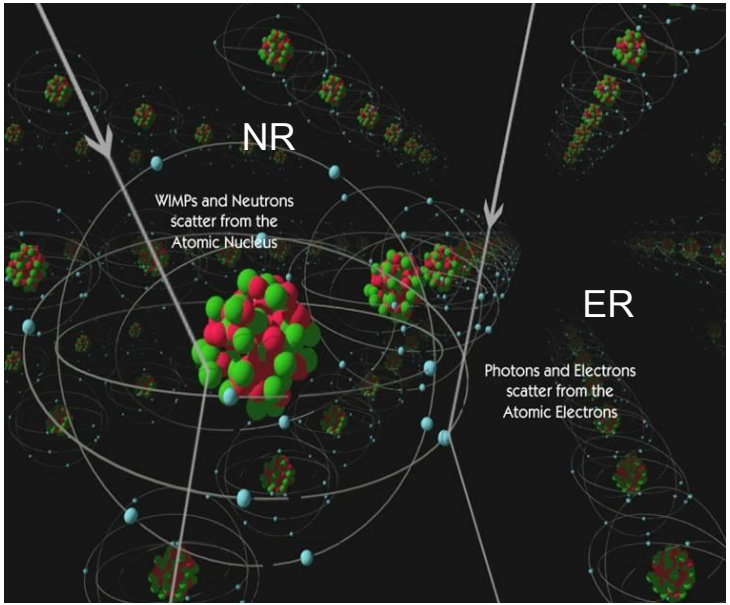

We focus on **ER** in this work because we can reliably identify a clean sample of **ER** events with well-known energy deposits from the real data, allowing us to generate a similar simulation sample for comparison.
(details will be shown later)

Phonon Generation in Germanium Crystal and Expected Total Phonon Energy

Simplified description of what happens inside the Ge crystal when an ER interaction occurs

- **Creation of electron-hole pairs**
  An ER interaction in the Ge crystal ionizes a number of electrons, leaving an equal number of holes, known as electron–hole pairs (referred to as charges or charge carriers in this work)

- **Neganov-Trofimov-Luke (NTL) Effect**
  In the electric field, charge carriers keep picking energy and colliding with the Ge lattice, generating a large number of lattice vibrations, also known as phonons (Luke phonons)
  This process enlarges the total energy initiated from a small energy deposit and gives the pulses a larger signal-to-noise ratio

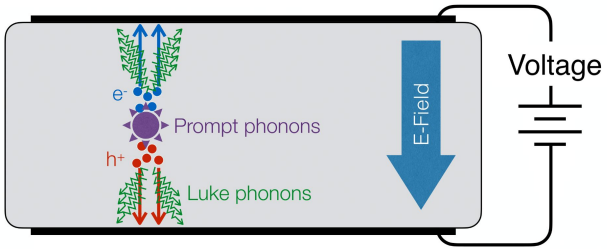

- **The expected total phonon energy**
  Can be quantified as the the sum of the initial energy deposit from the ER interaction (E_{ER}) and the energy carried by the Luke phonons (E_{NTL}), given by

$$E_{total} = E_{ER} + E_{NTL} = E_{ER} \times (1 + e\Delta V/E_{eh})$$

  - For CDMSlite, it is E_{total} / 2 as only one side is read out. E_{ER} = 10 keV ⇒ E_{total} / 2 = 123.24 keV

Mismeasurement Causes

The expectation is that there are four dominant processes by which the charges (e-/h^+) don't traverse the full voltage drop (70 V), thus generating less-than-expected phonon energy.

① Off-Electrode Effect

Some charges get absorbed by the detector surface away from the electrodes.

(It is a small but noticeable effect that impacts all events)

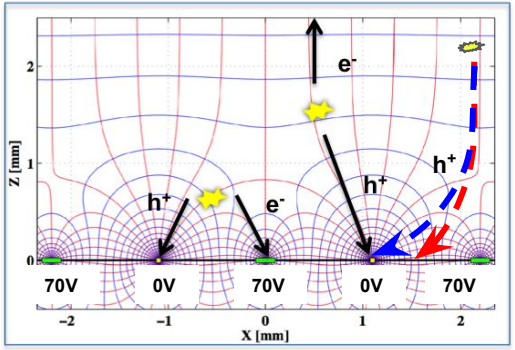

①

② Reduced Voltage

The voltage drop is <70V in a region near the detector sidewall, caused by grounded detector housing

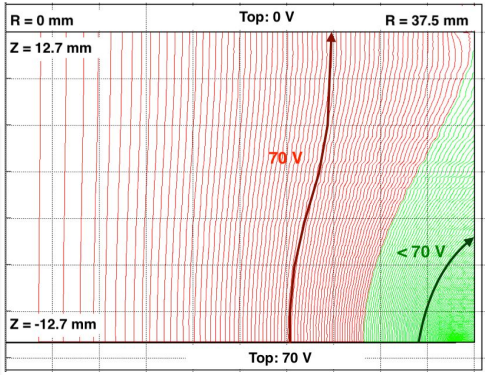

②

③ Surface Trapping

If an ER occurs very close to the surface, charges initially travel a short distance in random directions, some of which get absorbed before experiencing any voltage drop

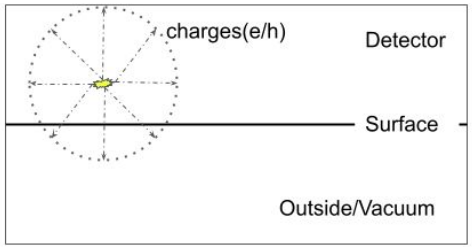

③

④ Sidewall Effects

If an ER occurs close to sidewall, some charges hit the sidewall and get absorbed before reaching the surface

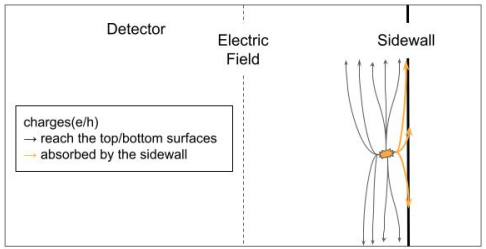

④

Expected Regions of Well- and Poorly-Measured Events

Since the four processes occur at specific regions, the expectation is that there are physical regions where events are well-measured (**Fiducial region**) and where events are poorly-measured (**Non-fiducial region**)

non-fiducial region (Surface Trapping)

non-fiducial region
(Sidewall Effects)

non-fiducial region
(Reduced Voltage + Sidewall Effects)

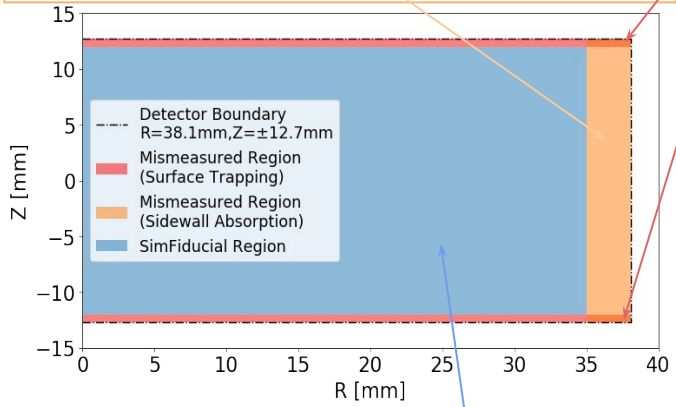

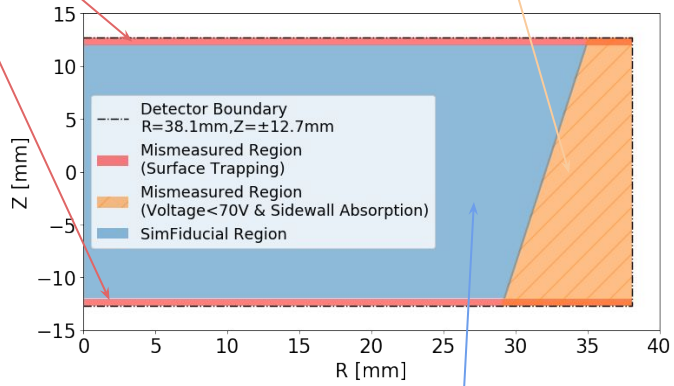

fiducial region, w/o Off-Electrode Effects, collecting ~100% of the expected total phonon energy

fiducial region, w/ Off-Electrode Effects, collecting a bit less than 100% of the expected total phonon energy

Phonon Transport before Absorption: Fast and Slow Components

- After generation, phonons can undergo multiple interactions before getting absorbed by QETs. The transport and reflection behaviors lead to phonon energy collection over an extended timescale (~ms).
- A simple macrophysical modeling: the phonon collection has the fast/slow components.

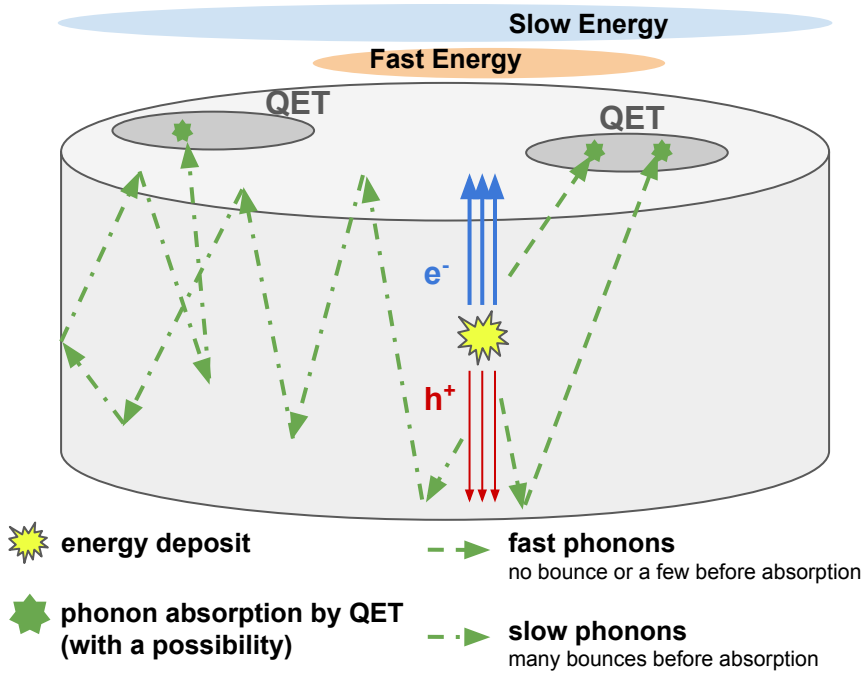

Fast phonons: with no or a few reflections, absorbed at earlier times

Fast Energy: energy carried by fast phonons, collected by QETs in a small region above the interaction position (orange circle).

Slow phonons: uniformly distributed inside the detector after many reflections, absorbed at later times

Slow Energy: energy carried by slow phonons, collected by QETs across the whole surface (blue circle).

A Simple Description of the Fast/Slow Energy Distributions: Two-Circle Model

Based on the regions where the fast and slow phonons are absorbed, the Fast/Slow Energy distributions can be described by a simplified two-circle model
(★: interaction position)

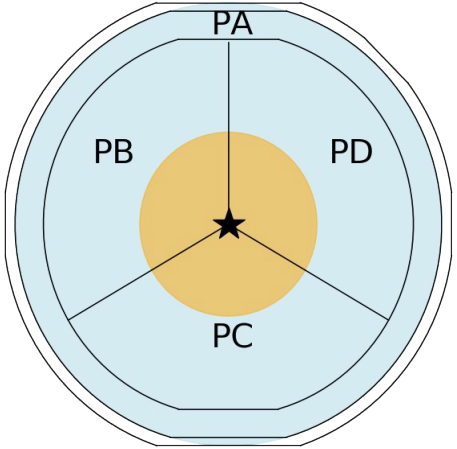

- **Fast Energy** distribution
  a orange circle with a smaller radius
- **Slow Energy** distribution
  a blue circle with the same radius as the detector

(A quantitative model will be shown in data analysis)

For use in data analysis, a useful labeling for the three inner channels:

- The **lead** channel collects the **most Fast Energy**
- The **near** channel collects **more Fast Energy**
- The **away** channel collects the **least Fast Energy**

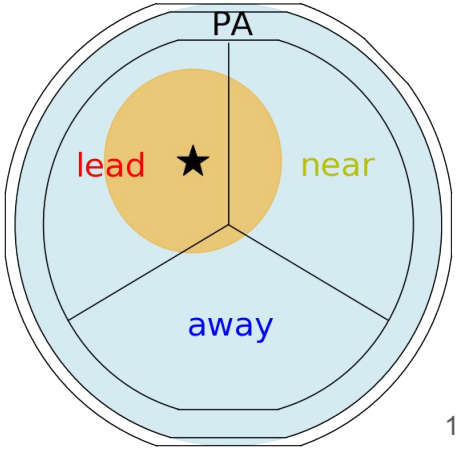

Superconducting Phonon Sensors Absorb Phonons and Produce Signals

An QET has an aluminum (Al) fin and a tungsten (W) wire integrated into a voltage circuit. At the operation temperature (~50 mK), the Al fin is in the superconducting state, and the W wire is in the transition edge

⓪ Initially, two electrons in the Al fin are weakly bound (Cooper pairs)

① Upon absorption of a phonon, Cooper pairs break into two quasiparticles and can diffuse into W wires

② Quasiparticles increase the temperature and resistance of W wires. As part of a circuit, this results in a measurable current response, known as signal or pulse

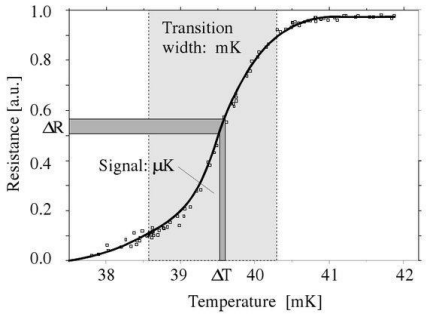

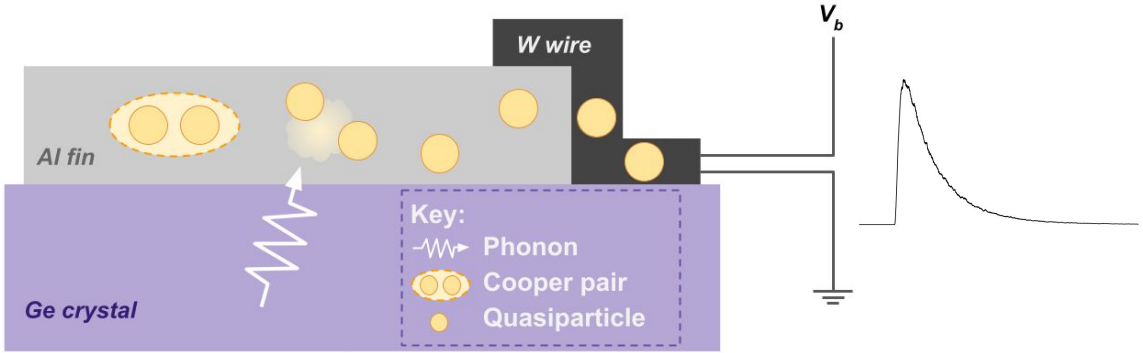

Expected Pulse Shape

We have expectations for the pulse shapes based on the collection of Fast/Slow Energy

- **Total Pulse**

  total pulse: summed pulse from all four phonon channels, PA+PB+PC+PD

  Previous analyses noticed that the total pulse usually has about the same shape: The average is referred to as ‘Average Template’

  We expect the total pulse to be consistent with Average Template assuming that the amounts of Fast/Slow Energy do not vary much as a function of interaction position

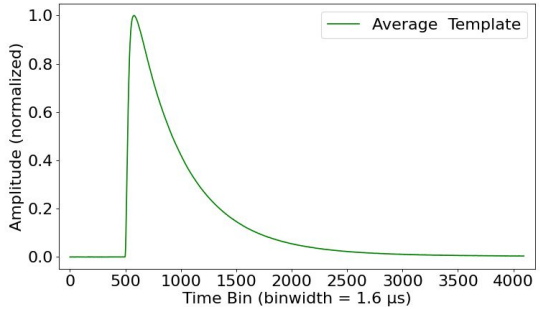

- **Individual/Combined Pulse**

  individual pulse: pulse from individual channel, PA/PB/PC/PD;
  outer pulse: pulse from the outer channel, PA
  inner pulse: pulse from the combined channels PB+PC+PD

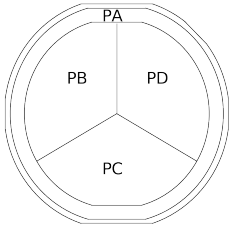

  Qualitatively, we expect the pulse to

  - rise more/less sharply and reach its maximum at an earlier/later time, when a channel collects more/less Fast Energy
  - have consistent falling portions at later time across channels as Slow Energy is evenly collected by all channels

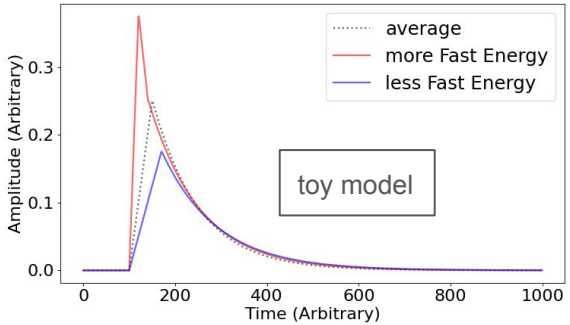

Outline

- **Introduction**
  - Evidence for Dark Matter and the WIMP Hypothesis
  - Overview of the SuperCDMS Soudan Experiment and the CDMSlite Detector
  - Thesis Goals
- **CDMSlite Detector Physics**
  - Electron Recoil Interactions
  - Detector's Response and Output
- **CDMSlite Experimental Data for this work**
- **SuperCDMS Simulation and CDMSlite Simulation Samples**
- **Data Analysis**
  - Collection Efficiency
  - Energy Collection over Position and Time
  - Simulation-based Analysis Methods using Pulse Shape Characteristics (Rejecting Poorly-Measured Events, Estimating Interaction Positions, Calibrating Real Pulses)
  - Comparison of Pulse Shapes between Simulated and Real Experiment Data
- **Future Work and Conclusions**

Main ER Source in CDMSlite: Photons and Electrons from Ge-71 Decay

Ge-71 is used for CDMSlite in-situ energy calibration. Ge-71 atoms releases three known energies (10.37, 1.3, 0.16 keV) via electron capture decay by emitting photons and electrons

- Ge-71 is produced by Ge-70 (~20% natural abundance) in the Ge crystal capturing a neutron from the neutron source Cf-252 placed nearby the CDMSlite detector

  $$\text{Ge-70} + n \rightarrow \text{Ge-71}$$

- Ge-71 atoms undergoes electron capture decay (with a half life of 11.43 days), emitting photons and electrons with energies equal to the binding energy of electrons

  $$\text{Ge-71} + e \rightarrow \text{Ga-71}^* \rightarrow \text{Ga-71} + \gamma, e$$

Shell	Probability of Electron Capture (Ge-71)	Binding Energy (Ga-71) [keV]
K	87.59%	10.367
L	10.49%	1.299
M	1.92%	0.160
N	neglected	no data

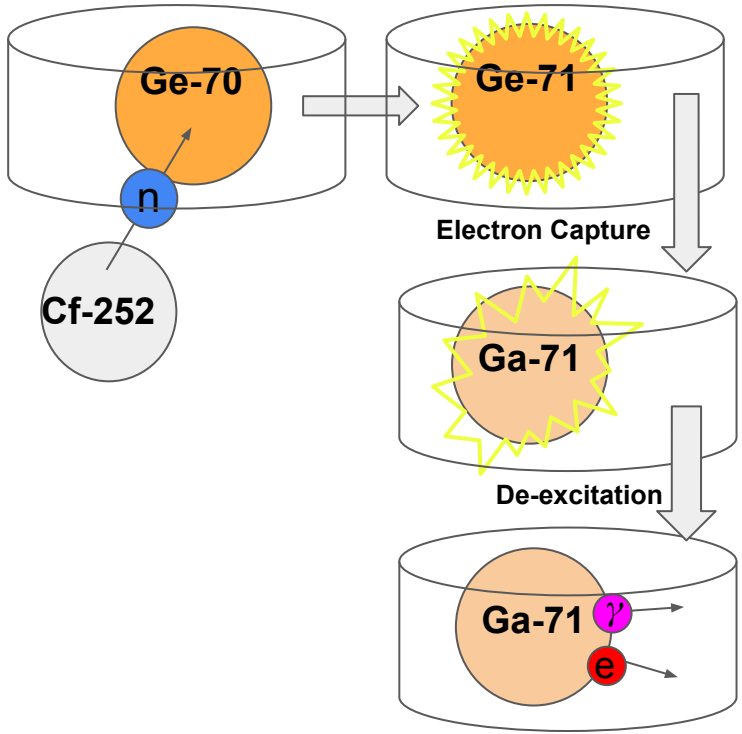

The Experimental Dataset Selected for this Work

We choose the events in the CDMSlite real data that have the total phonon energy within the largest peak in the energy spectrum, which has the largest statistics.

- The best-fit amplitudes of total pulses, PTNFamps, from the previous CDMSlite analysis are used as the energy estimator, assumed to be proportional to the total phonon energy
  (plot: the PTNFampls distribution with the range over the three peaks from Ge-71 decay)
- Using the 2σ criterion from a Gaussian fit, we select events within the dominant peak corresponding to the 10.37 keV line from the Ge-71 decay
  (as shown in the plot below)

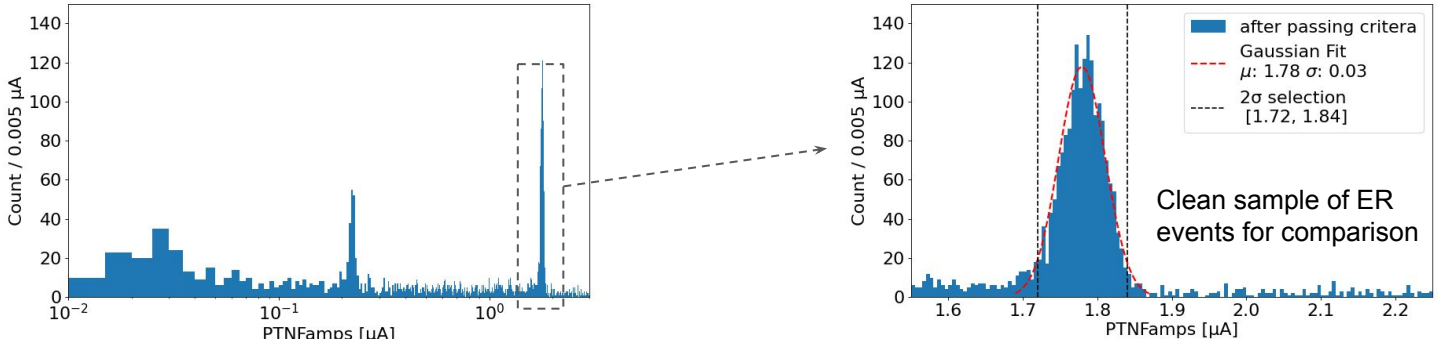

Outline

- **Introduction**
  - Evidence for Dark Matter and the WIMP Hypothesis
  - Overview of the SuperCDMS Soudan Experiment and the CDMSlite Detector
  - Thesis Goals
- **CDMSlite Detector Physics**
  - Electron Recoil Interactions
  - Detector's Response and Output
- **CDMSlite Experimental Data for this work**
- **SuperCDMS Simulation and CDMSlite Simulation Samples**
- **Data Analysis**
  - Collection Efficiency
  - Energy Collection over Position and Time
  - Simulation-based Analysis Methods using Pulse Shape Characteristics (Rejecting Poorly-Measured Events, Estimating Interaction Positions, Channel-by-Channel Relative Calibration)
  - Comparison of Pulse Shapes between Simulated and Real Experiment Data
- **Future Work and Conclusions**

CDMSlite Simulation and SuperCDMS Simulation Infrastructure

With the understanding of the detector physics underlying the CDMSlite detector response to ERs, we are able to use the SuperCDMS simulation tools to produce results for comparison

Source Simulation (SourceSim)

simulates pure ERs with single 10 keV energy deposits inside the CDMSlite detector to mimic the interactions from photons/electrons

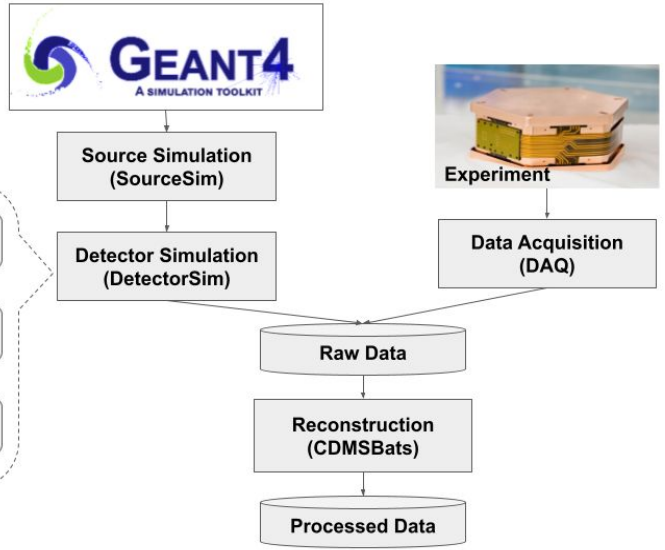

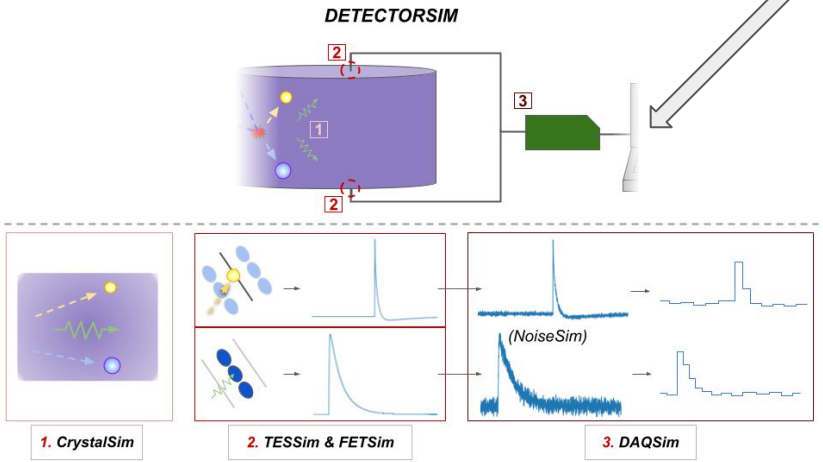

Detector Simulation (DetectorSim)

- CrystalSim simulates creation of e-h pairs and phonon transport and reflections inside the detector
- TESSim simulates the QETs' response upon phonon absorption to produces signals
- DAQSim converts the signals to pulses with the same format as the real data (Raw Data)

Motivation for CDMSlite Simulation

In order to answer the questions we asked on Slide 9, we consider a series of analyses as listed below and create three simulation samples (next page) for this work.

- **Collection of total phonon energy**
  ⇒ “Can we reproduce the expected energy inside the detector in our simulation as well as the dominant mismeasurement causes?”
- **Phonon energy collection over position and time**
  ⇒ “Are the previous models to describe the macroscopic output from billions of microphysical interactions well-justified? Can they be made better?”
- **Development of new analysis methods based on pulse shape characterizations**
  ⇒ “Are the previous assumptions about the correlation between interaction positions in the detector and its signal pulses justified?
  ⇒ Does the simulation suggest new methods to improve analysis (e.g. rejecting poorly-measured methods, estimating interaction positions, calibrating pulse scalings)?”
- **Comparison pulse shape characterizations between simulated and real data**
  ⇒ “How well does the current version of the simulation reproduce what we see in the real data?”

Simulation Samples Produced for This Work

UniE sample

- uniform electric field without electrodes
- 1000 events uniformly distributed inside detector
- output: phonon energy collected by each channel

EPot sample

- realistic electric field model with electrodes
- 1000 events uniformly distributed inside detector
- output: phonon energy collected by each channel; pulses out of channels

EPot_hits sample

- realistic electric field model with electrodes
- only 1 event at the detector center
- output: time/position/energy information of each phonon absorption

Outline

- **Introduction**
  - Evidence for Dark Matter and the WIMP Hypothesis
  - Overview of the SuperCDMS Soudan Experiment and the CDMSlite Detector
  - Thesis Goals
- **CDMSlite Detector Physics**
  - Electron Recoil Interactions
  - Detector's Response and Output
- **CDMSlite Experimental Data for this work**
- **SuperCDMS Simulation and CDMSlite Simulation Samples**
- **Data Analysis**
  - Collection Efficiency
  - Energy Collection over Position and Time
  - Simulation-based Analysis Methods using Pulse Shape Characteristics (Rejecting Poorly-Measured Events, Estimating Interaction Positions, Calibrating Real Pulses)
  - Comparison of Pulse Shapes between Simulated and Real Experiment Data
- **Future Work and Conclusions**

Compare Collected Phonon Energy to the Expected Value

- Expected total phonon energy: 123.24 keV (see Slide 12)
- Collection Efficiency: Collected / Expected (e.g. collected 100 keV, collection efficiency = 100/123.24 = 0.8114)

Due to a large Fiducial Region and a smaller Non-Fiducial Region (see Slide 14), for both UniE and EPot samples, there is a large peak on the right and a long tail on the left

UniE sample

- Peak ($\mu \pm \sigma$): 0.9994 ± 0.0064

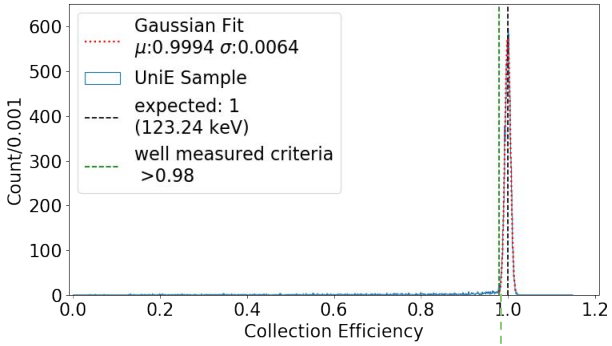

Poorly-measured events
< 0.98 (3σ)

Well-measured events
≥ 0.98 (3σ)

EPot sample

- Peak ($\mu \pm \sigma$): 0.9805 ± 0.0098
  (2% less than UniE due to off-electrode effects)

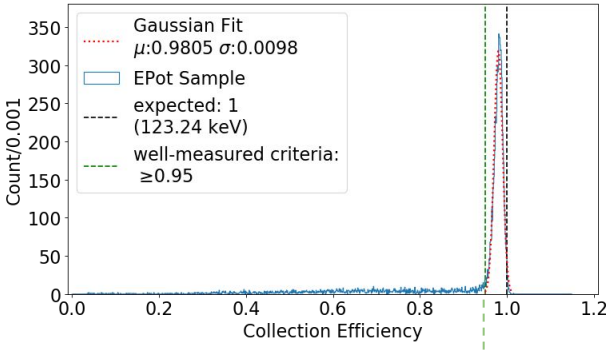

Poorly-measured events
< 0.95 (3σ)

Well-measured events
≥ 0.95 (3σ)

Compare Regions of Well- and Poorly-Measured Events to Expectations

With criteria of well-measured events established, we are able to see where both well- and poorly-measured events occur. The results are consistent with our expected Fiducial and Non-Fiducial Regions (see Slide 14).

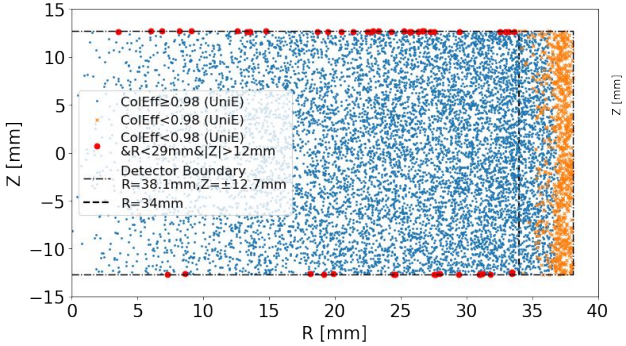

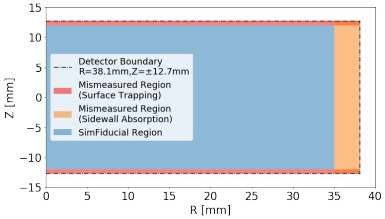

UniE sample

Non-Fiducial Regions

- |Z| > 12mm, affected by surface trapping
- R > 37 mm, influenced by sidewall effects (some at 34 < R < 37 mm due to the flats of the CDMSlite detector)

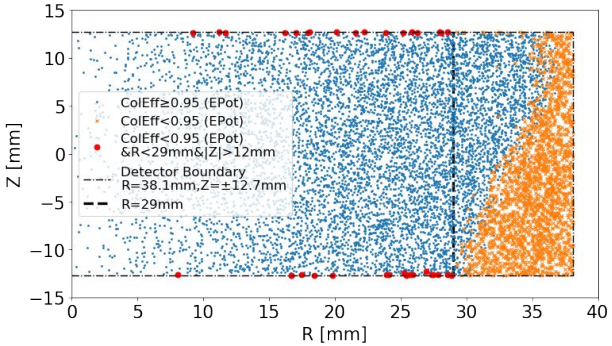

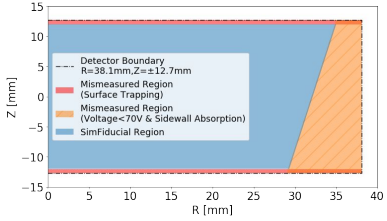

EPot sample

Non-Fiducial Regions

In addition to the same regions as in the UniE sample,

- A triangle-like area with the lower edge extending to R = ~ 29 mm, influenced by the reduced voltage.

Overview of Phonon Energy Collection over Position and Time: EPot_hits sample

Phonon energy collection by QETs over time
(note: not including the QETs' response)

- Rises quickly after the energy deposit

  Corresponding to the absorption of fast phonons
- Falls gradually over time

  Corresponding to the absorption of slow phonons that decrease over time inside the detector

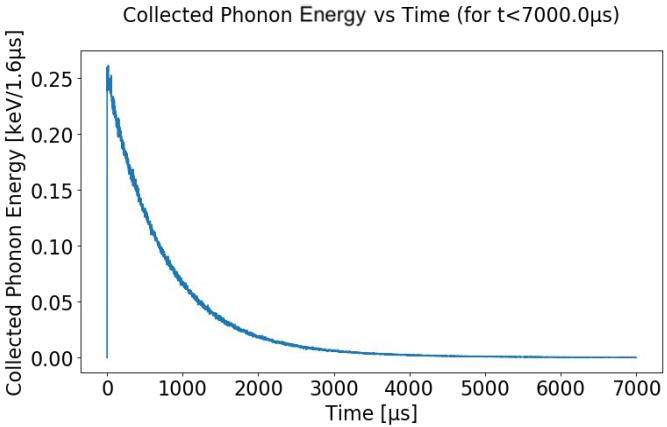

To produce a quantitative macroscopic model for the phonon energy collection over time, we need a simple way to determine how phonon absorption positions change over time

- QETs are not uniformly spaced so we select a region between the channels (|X| < 2 mm and Y > 0 mm) where the QETs are arranged radially: Allows us to estimate the response as a function of R (using Y to indicate R)

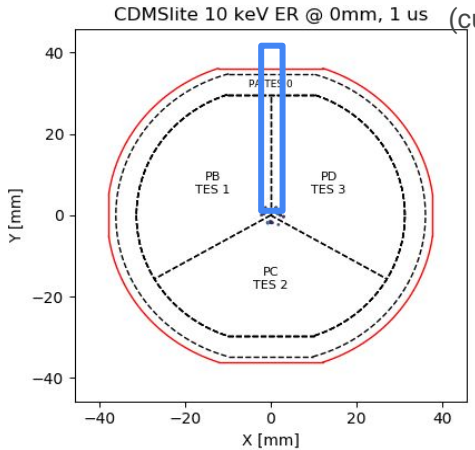

The first phonons absorbed right after t=0 by a few sensors above the interaction.

The absorption positions then spread out over time

Phonon Absorption Position Distribution (Radial Direction) over Time

We quantify the phonon absorption positions changing over time (t< 500 μs) by the selected sensors. Here we show the average (mean) and root-mean-square (RMS) for every 2 μs.

- The mean and RMS increase over time and approach constants
- Both exceed 90% of their respective maxima at 100 μs
  - indicating that the remaining phonons in the detector become nearly uniformly distributed at this point
- So, we separate Fast and Slow Energy by 100 μs

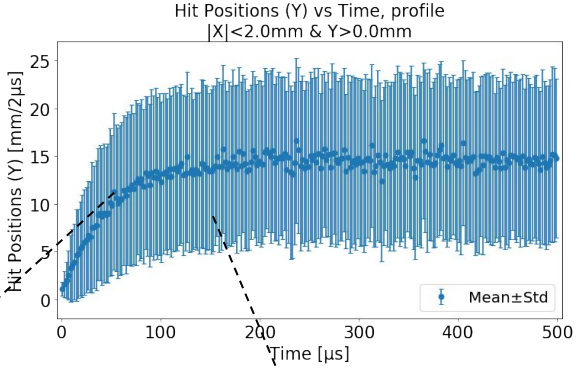

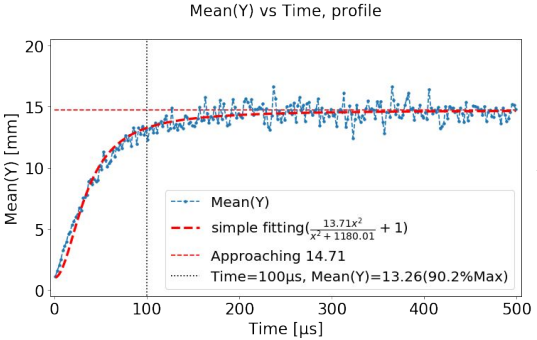

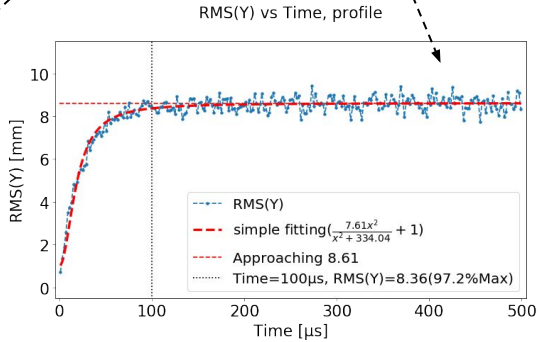

Modeling the Spatial Distribution of Fast and Slow Energy

With a clean time separation, we are able to move forward from the qualitative two-circle model (slide 16) to a quantitative, and a physically well-motivated model

⓪ The distribution of phonon energy collected by the selected sensors

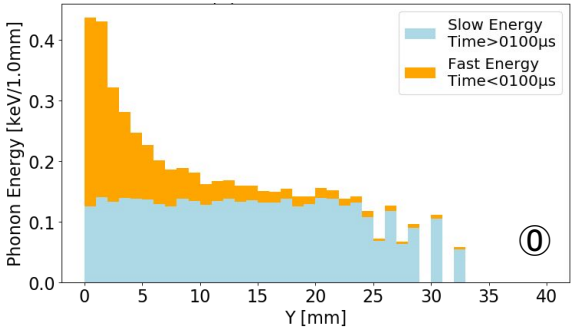

① Mimic the phonon energy distribution along the whole diameter for easier visualization by mirroring the distribution around Y=0.

The Fast Energy distribution: Gaussian-like profile,

The Slow Energy distribution appears nearly uniform

② Fit a generalized Gaussian for the Fast Energy distribution

$$f(y) = A \cdot \exp\left(|y - \mu| / \alpha\right)^{\beta}$$

Where A = 0.4, μ = 0, α = 3.5, and β = 0.8

③ The Fast and Slow Energy distributions from the top view by extrapolation

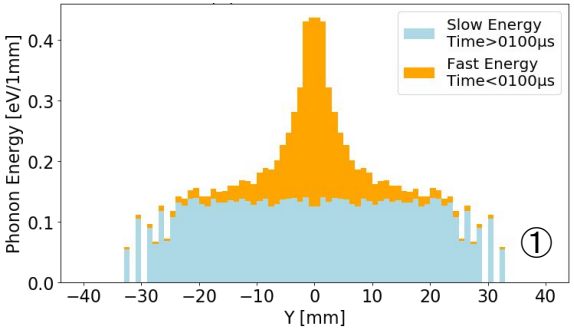

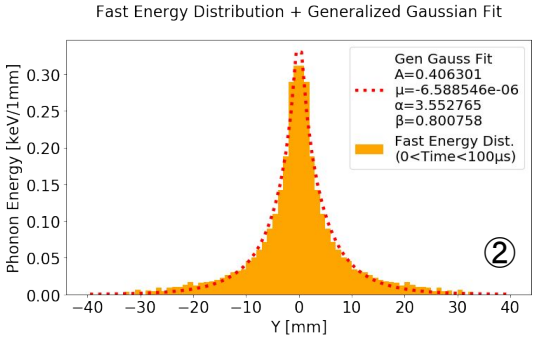

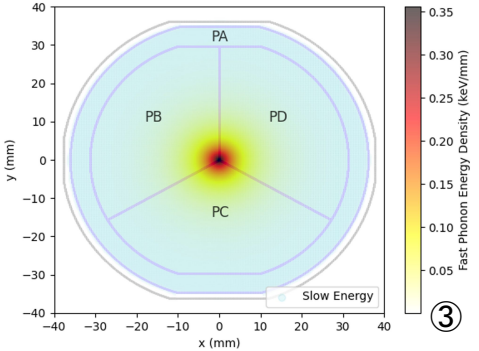

Overview of Pulse Shape, Individual Channels Collecting Different Fast Energy

- Since the phonon collection over time appears to be well-modeled by fast and slow components, we next move to develop new analysis methods for use in real data
- We construct quantities directly from the simulated pulses (EPot sample) that are available in real pulses.
- We focus on the quantities from the early and late portion of pulses

- Early portion:
  Different rising shape and peak vicinity
  When a channel, or combined channels, collects more Fast Energy, the pulse has
  - a larger pulse value at an early time bin
  - a higher maximum at an earlier time bin

- Tail Portion:
  Consistent falling shape
  - Individual channels have the same area and number of QETs
  - Expect the Slow Energy to give consistent pulse values at later times

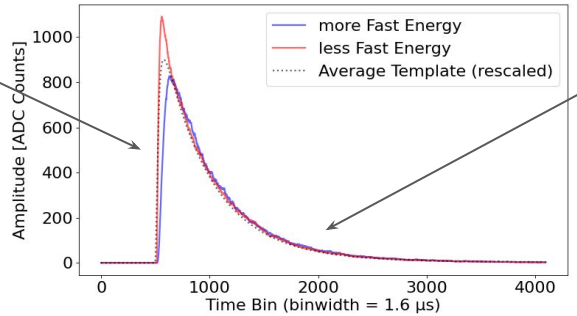

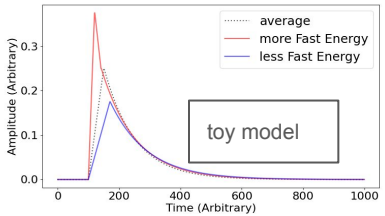

Qualitative expected shape from slide 18

Useful Sets of Pulse Shape Quantities for use in Characterization

Quantities constructed from the early portion of pulses

- ***Val542***
  the pulse value at bin 542
  (542 is picked from a study on Peak Bin for the lead channel. More soon)
- ***Peak Bin***
  the time bin at which the pulse reaches its maximum
- ***Peak Value***
  the maximum value of a pulse

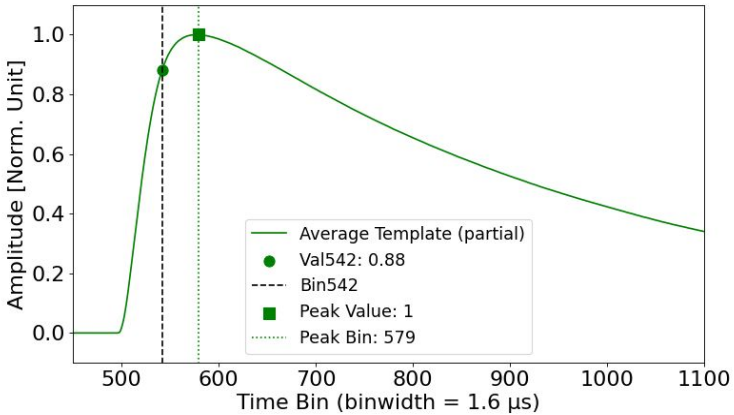

Quantities constructed from the tail portion of pulses

The tail region is defined as t > 2ms (bin 1250) and is fitted with a exponential function, $A \cdot \exp(-(t - 2) / \tau)$

- ***Value@2ms*** (the pulse value at 2 ms or bin 1250)
- ***Tail Amplitude*** (A)
- ***Fall Time*** (τ)
- ***Integral Area***: $A\tau$

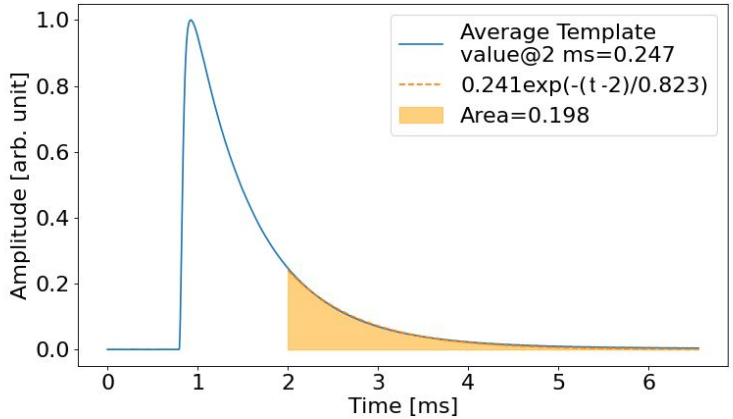

Predictions and Expectations for Variation of Quantities

The **Fast Energy** sharing among channels determine the variations of the early-portion quantities ***Val542***, ***Peak Bin*** and ***Peak Value***. We expect

- the largest variation with interaction positions for the lead channel as it collects the most Fast Energy.
- the variation as a function of R only between the outer channel (PA) and combined inner channels (PB+PC+PD)
- the variation as a function of |ΔΦ| with R fixed between the lead and near channel
  (|ΔΦ|: angular difference between the interaction position and the lead channel center)

We expect that the **Slow Energy** is evenly collectly by all channels due to the same number of QETs in each, so that we expect the values of the tail-portion quantities (***Value@2ms***, ***Tail Amplitude***, ***Fall Time*** and ***Integral Area***) to be consistent between channels

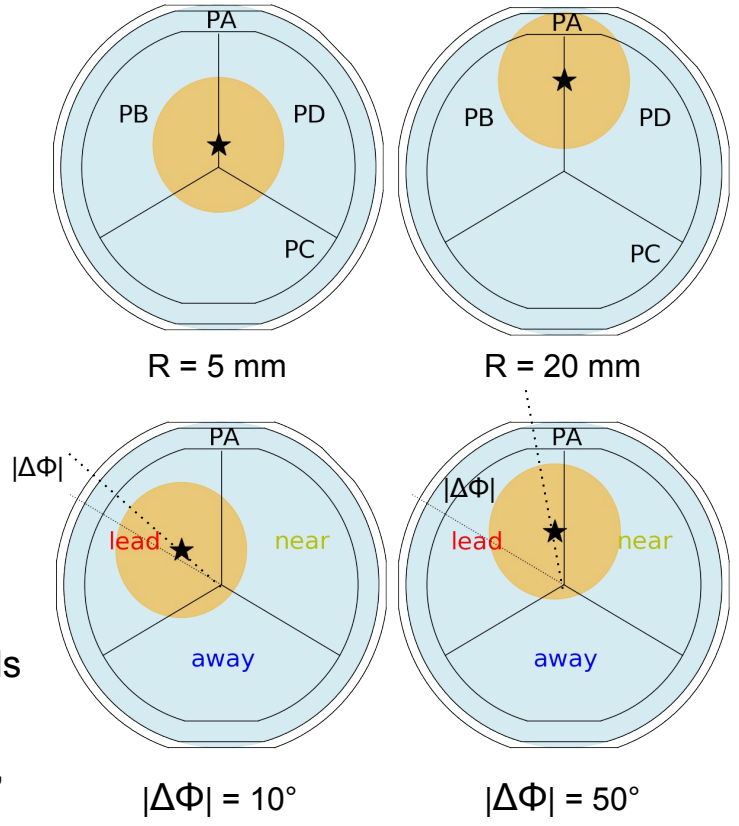

Overview of How We Use the Pulse Shape Quantities for the Rest of the Analysis*

We use the quantities to develop new analysis methods and compare simulations (EPot sample) to expectations and real data to answer our questions with 3 main tasks.

1) We use the early-portion quantities to
   a) Reject poorly-measure events in simulation
   b) Estimate interaction positions (R and $|\Delta\Phi|$) of the well-measured events in simulation

2) We use the tail-portion quantities to
   a) Test the assumption of "all channels should have the same tail"
   b) Calibrate the real pulse using the distributions of the quantity values

3) We compare the simulated pulses to real ones after calibration to see
   a) how well the simulation results compare to expectations as a function of position
   b) how well the distributions of the early-portion quantity values in simulated pulses reproduce those in real pulses (we don't know true position for real data)

* More details about all of these in Chapters 8, 9 and 10 respectively

Task 1A: Separating Well- and Poorly-Measured Events, using $PeakBin_{lead}$

We will only show a single example rejection technique. Most poorly-measured events occurs at large radius (R > 29 mm) due to the reduced voltage near the detector sidewall. **$PeakBin_{lead}$** is expected to have the largest variation with interaction positions, we expect it to separate well- and poorly-measured events in simulation (EPot sample)

- **$PeakBin_{lead}$**
  - around 542 for R < 25 mm and then rises for well-measured events (blue) (here is why we picked 542 for this work)
  - > 562 for most poorly-measured events (yellow)
- Separation criterion
  - Accept: 534 ≤ **$PeakBin_{lead}$** ≤ 562
  - Reject: **$PeakBin_{lead}$** < 534 or > 562
- Results:
  - 98.8% of the poorly-measured events are rejected
  - 75.4% of the well-measured events are retained

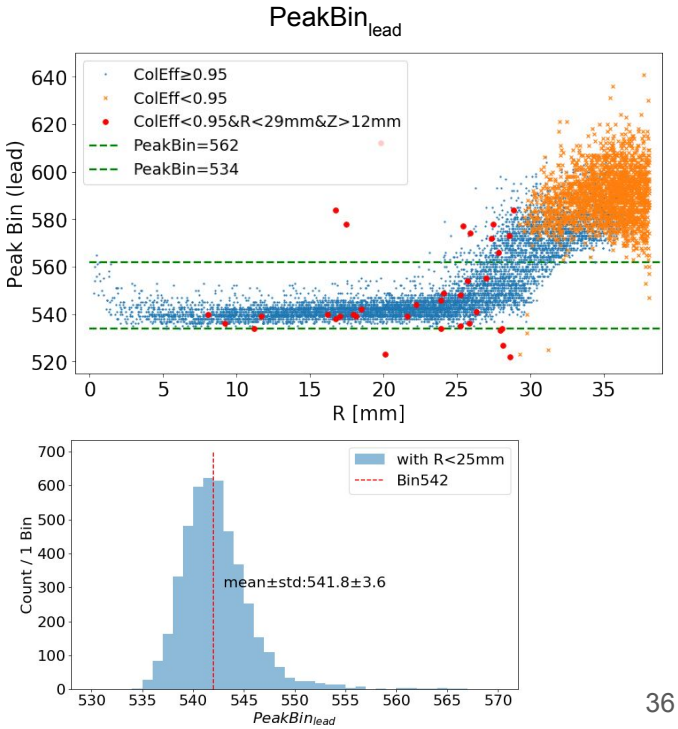

Task 1B: Estimating Interaction Positions (R) using $Val542_A/Val542_{BCD}$

Since we expect that the Fast Energy sharing in the outer and inner channels varies with R, we choose the **$Val542_A/Val542_{BCD}$** to estimate R for well-measured events in simulation (EPot sample).

- The average (mean) and root mean square (RMS) of **$Val542_A/Val542_{BCD}$** values vary as a function of R

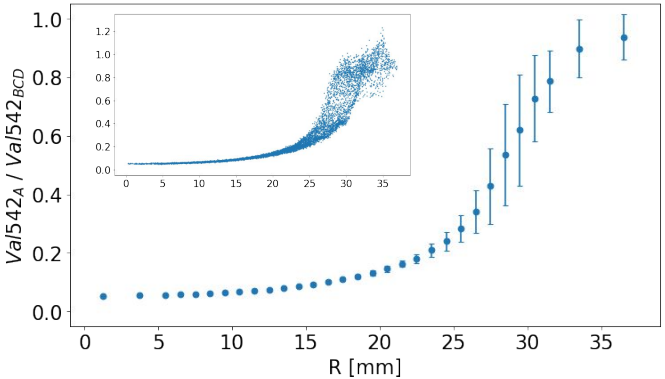

- Estimate R using linear interpolation of the mean values

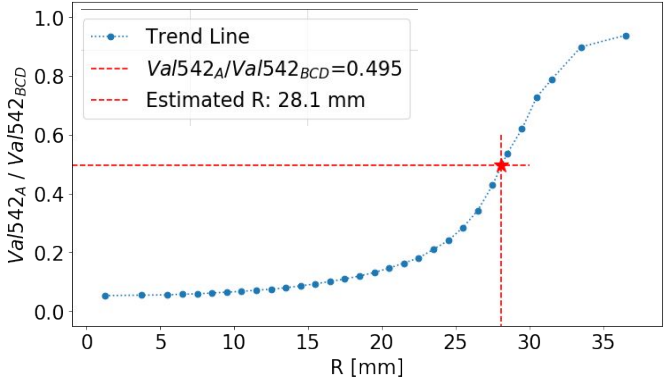

Estimated R (R_{est}) and Comparison to True Values (R_{true})

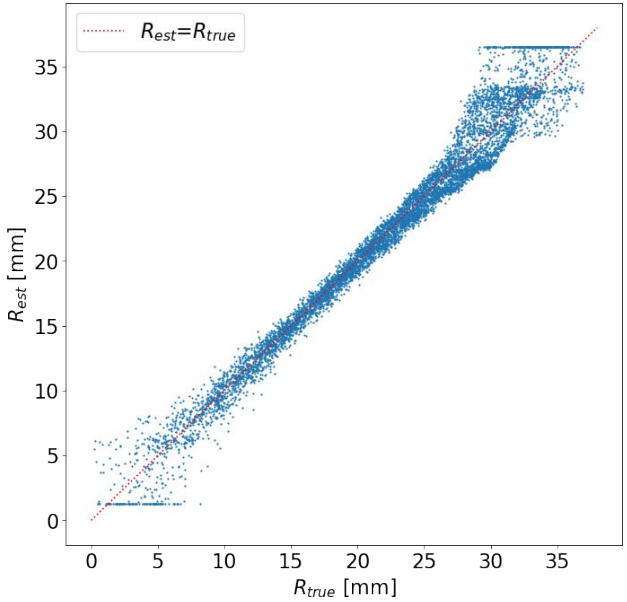

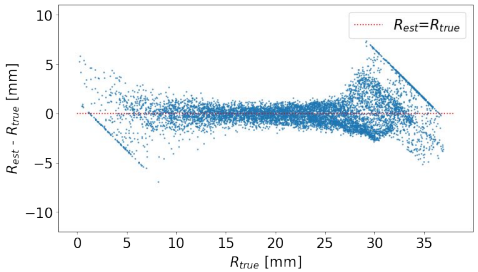

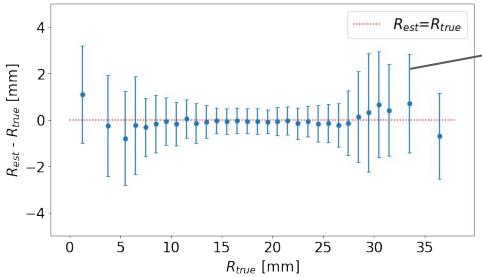

These plots show that the method allows for a fidelity measurement of R, although the resolution depends on the value of R.

- 1.0 - 2.0 mm for small R_{true} (<10mm)
- 0.5 - 1.0 mm for medium R_{true} (10 - 27 mm)
- 1.0 - 2.5 mm for large R_{true} (>27mm)

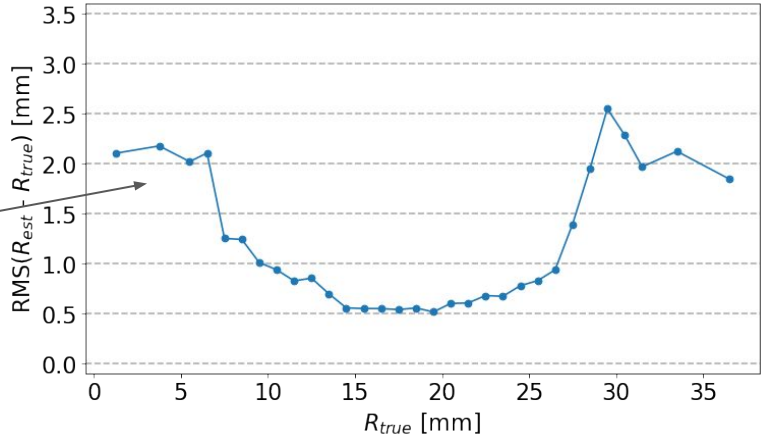

Task 1B: Estimating Interaction Positions (|ΔΦ|) using $Val542_{lead}/Val542_{near}$

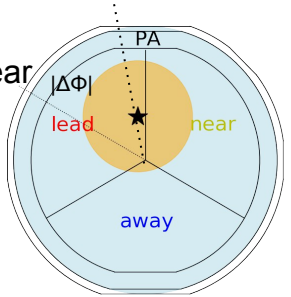

Since we expect that the Fast Energy sharing between the lead and near channel varies with both R and |ΔΦ|, we choose **$Val542_{lead}/Val542_{near}$** to |ΔΦ| with R_{est} for well-measured events in simulation (EPot sample).

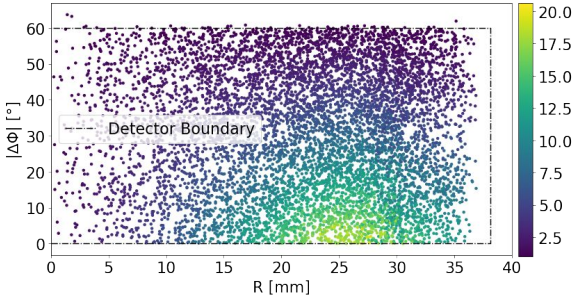

$Val542_{lead}$ / $Val542_{near}$ in R|ΔΦ|

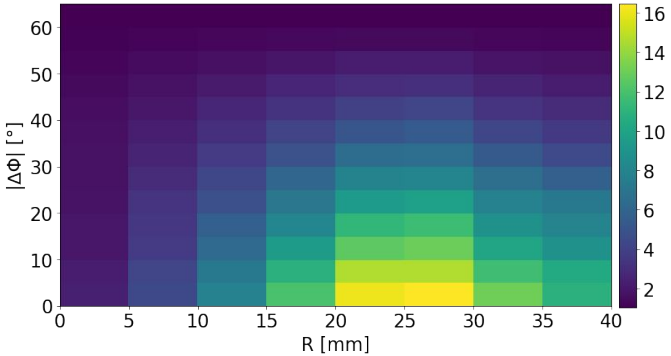

- The average (mean) of **$Val542_{lead}/Val542_{near}$** values vary as a function of R and |ΔΦ|
- Create a new trend line for R_{est} and then estimate |ΔΦ| using linear interpolation

$Val542_{lead}$ / $Val542_{near}$ vs |ΔΦ| with fixed R

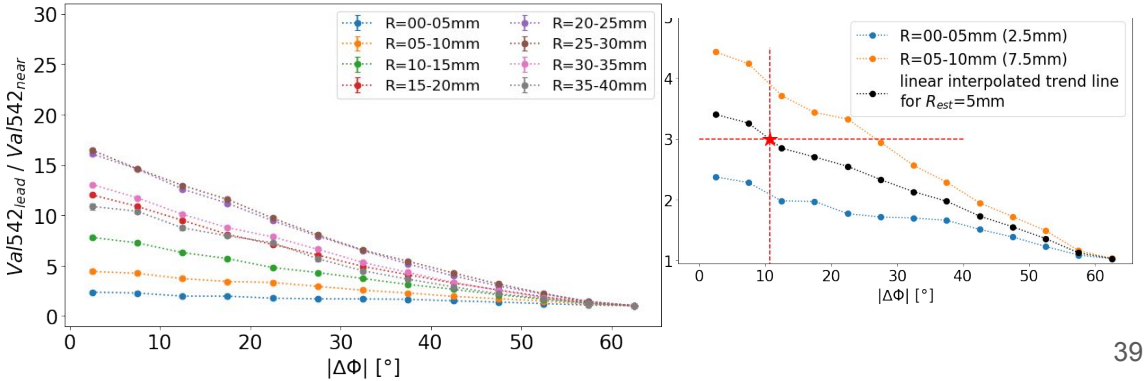

Estimated $|\Delta\Phi|$ ($|\Delta\Phi|_{est}$) and Comparison to True Values ($|\Delta\Phi|_{true}$)

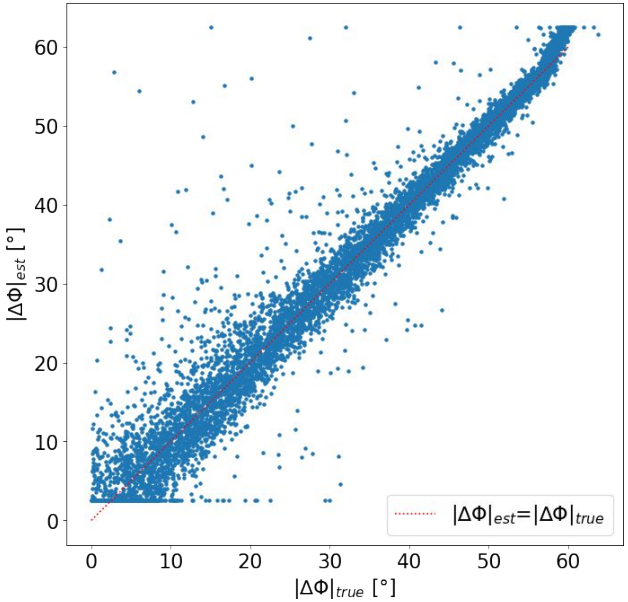

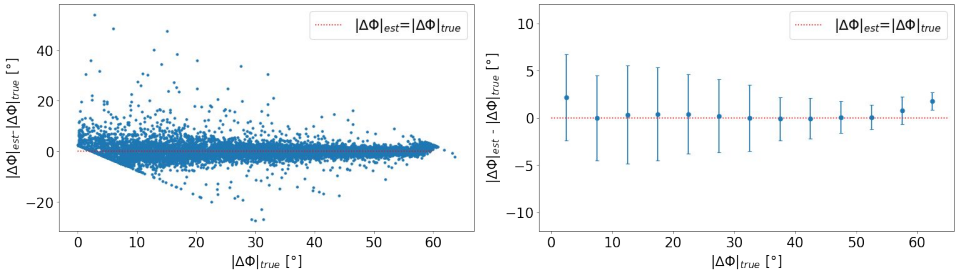

These plots show that the method allows for a fidelity measurement of $|\Delta\Phi|$, although the resolution depends on the value of $|\Delta\Phi|$

- ~5° for small $|\Delta\Phi|_{true}$ (< 20°)
  (near the center of the lead channel)
- Down to ~1° as $|\Delta\Phi|_{true}$ increases
  (close to the boundary of the lead and near channels)

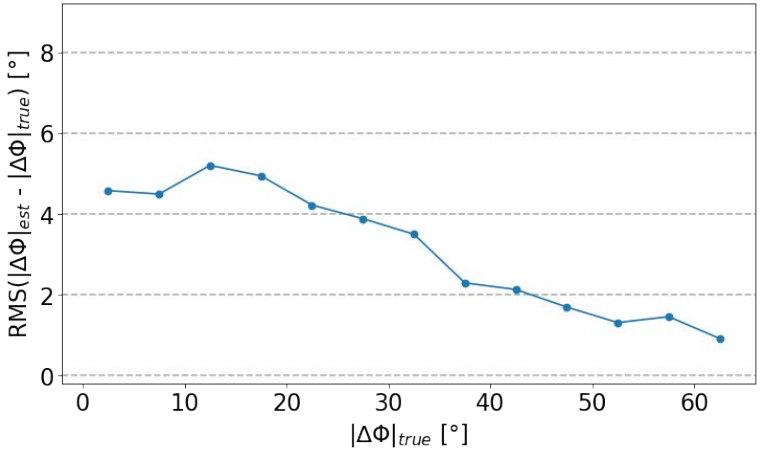

Task 2: Pulse Tail Study and Channel-by-Channel Relative Calibration

Let's move forward to the comparison of tails of simulated (EPot sample) and real pulses.

Motivation

- **In experiment**, there are differences in hardware and electronics associated with each channel, resulting in different scalings that can be seen in the pulse tails.
- **Ideally**, like in simulation there are no such differences, so the pulse tails are expected to be consistent with each other as the Slow Energy is evenly collected by channels.

Methods (Pulse Tail Study)

- We measured the values of the four pulse tail quantities (***Value@2ms***, ***Tail Amplitude***, ***Fall Time***, ***Integral Area***) for both simulated and real data
- Compare simulated and real pulses along with expectations.

Goals

- To justify the simple assumptions above
- Calibrate the real pulses for use in the comparison of the early portion of simulated and real pulses

A Quick Look at Example Simulated Pulses and Real Pulses

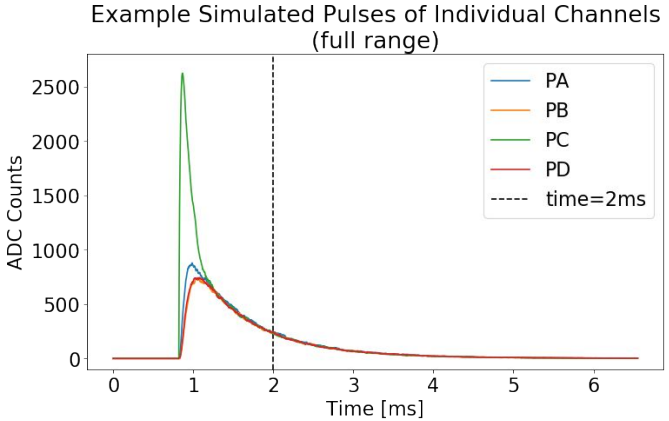

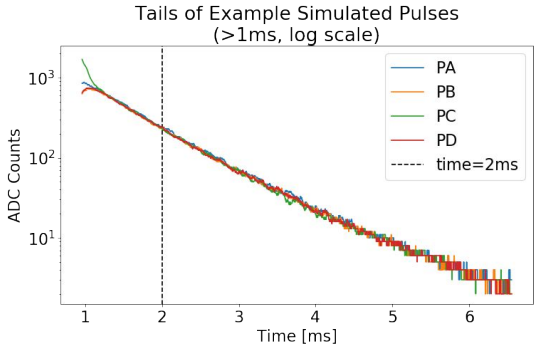

Note: no noise in simulation for this work

- overlapping tails → consistent scaling between channels

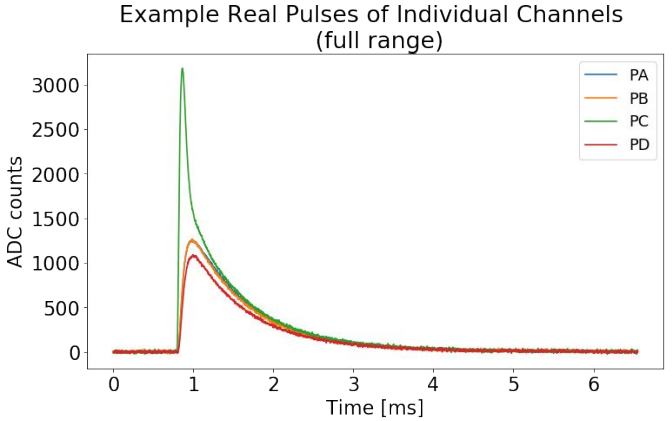

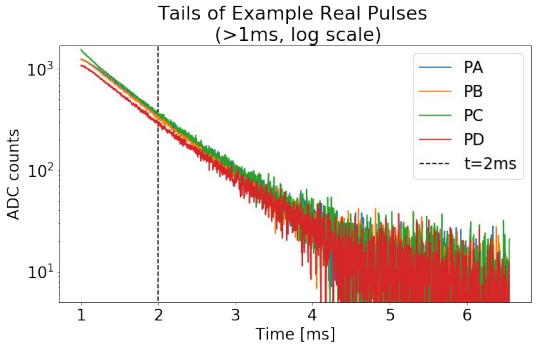

Fluctuation from the real-world noise

- separating tails → different scaling between channels

Results of Pulse Tail Study, using Tail Amplitude

The value distributions of tail-portion quantities have some consistency with the expectations, but also a significant difference. The full set of plots for the pulse tail study is shown on Slide 64 and Slide 65.

Here we use ***Tail Amplitude*** to discuss the main findings.

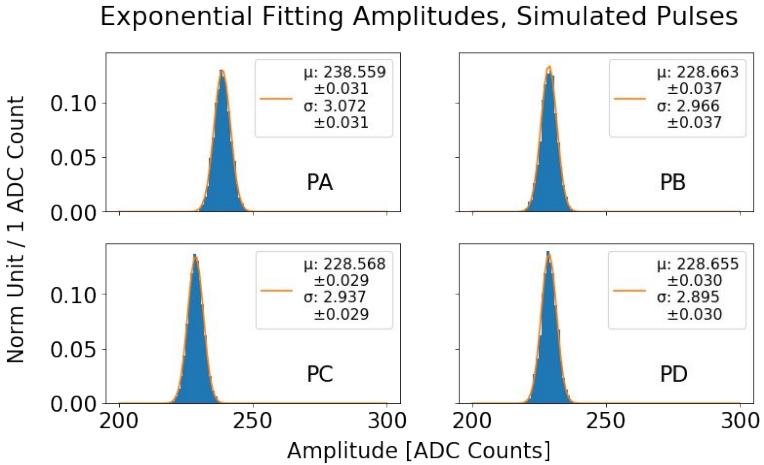

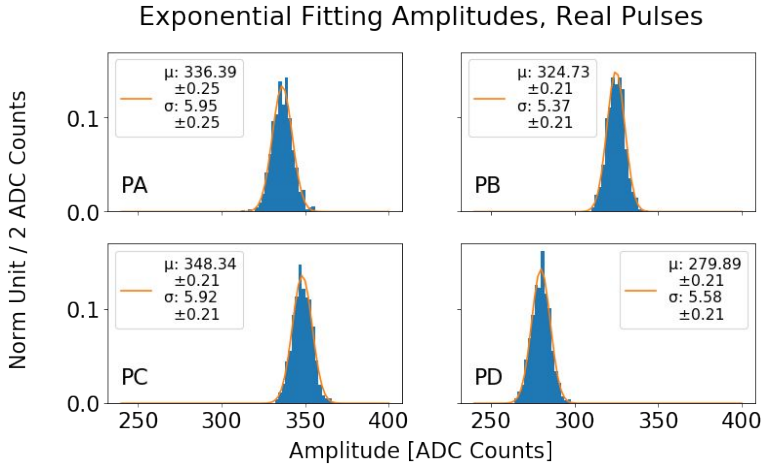

- PB/PC/PD: consistent mean values
- PA: a slightly higher (10 ADC counts) mean value, but it is statistically significant

- Inconsistent between channels

What We Learned from the Pulse Tail Study for us to Move Forward

- Two primary observations:
  - Simulated pulses: the inner channels (PB/PC/PD) behave identically within uncertainties, but the outer channel (PA) has small but significant differences for reasons not fully understood yet.
  - Real pulses: all channels behave significantly differently from each other as expected from differences in hardware and electronics (difficult to draw conclusions from this)
- This suggests two things:
  - The assumption that the real data can be calibrated by assuming all four channels have identical tails appears to not be well-justified
  - We have to choose a calibration method for our work. We choose to assume our simulation has it correct moving forward.
- Calibration: We scale the pulse from each channel in real data to match its corresponding channel in simulation

A Quick Look at Example Simulated and Real Pulses after Relative Calibration

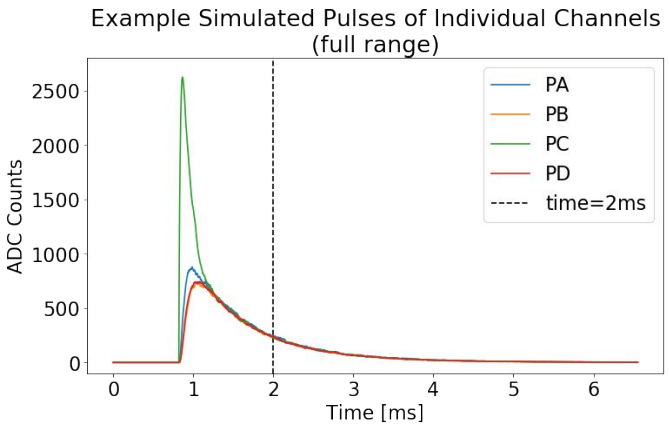

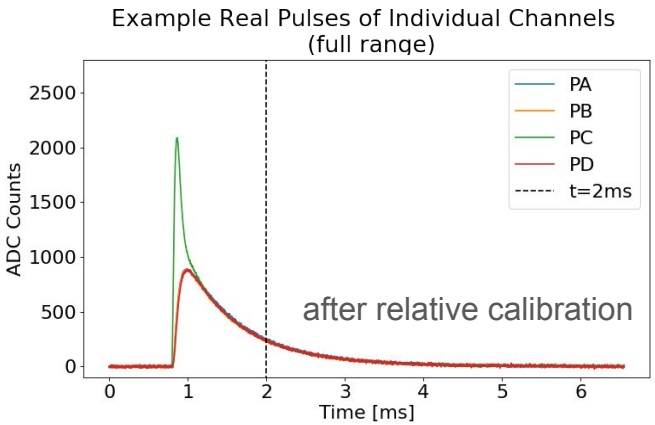

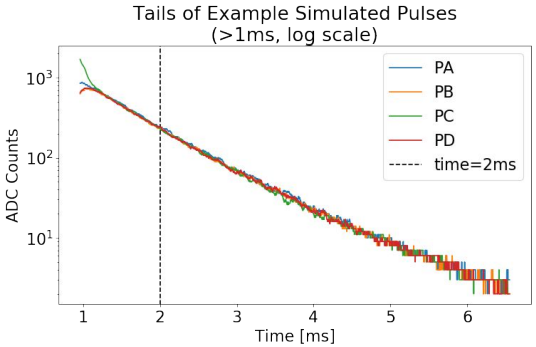

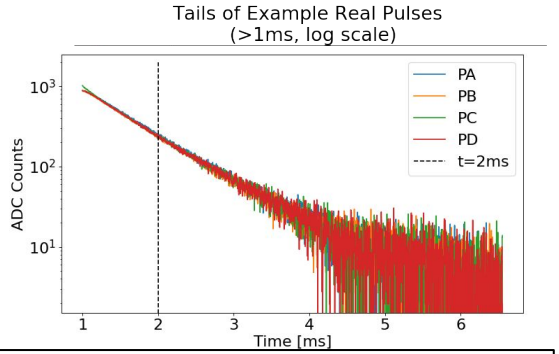

Note: no noise in simulation for this work

Fluctuation from the real-world noise

Simulated and real pulses are quite similar after calibration. There is qualitative agreement, but lingering quantitative differences

Task 3: Comparison of Simulated Pulses to Real Pulses after Relative Calibration

- Since the early-portion pulse quantities are more sensitive to position differences and whether the event is well-measured, we compare them for this task.
- We see see qualitative agreement, but quantitative differences.
  (example pulses and Average Template is used for illustration)

Qualitative Agreement

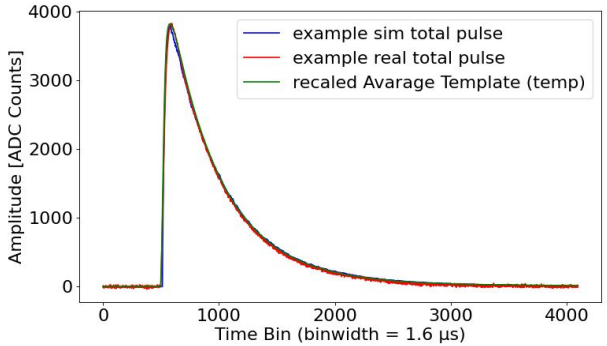

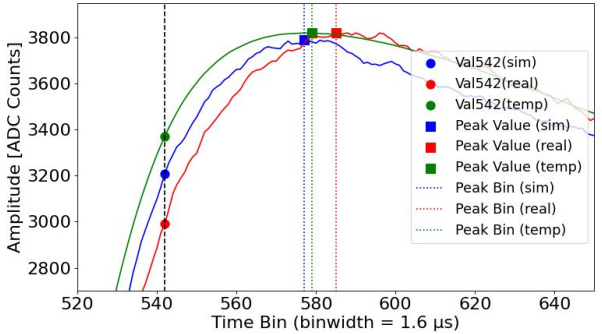

Quantitative Differences

Comparisons are made using quantities from total pulse, outer and inner pulse, individual pulse between

the simulated pulses (‘sim’) vs. **the real pulses after relative calibration (‘real’)**

Note: We only show the most revealing plots on the next pages with notes on each to help point the way forward to understanding the problems and next steps for future analyzers

Comparison, Total Pulse, Peak Value vs Peak Bin

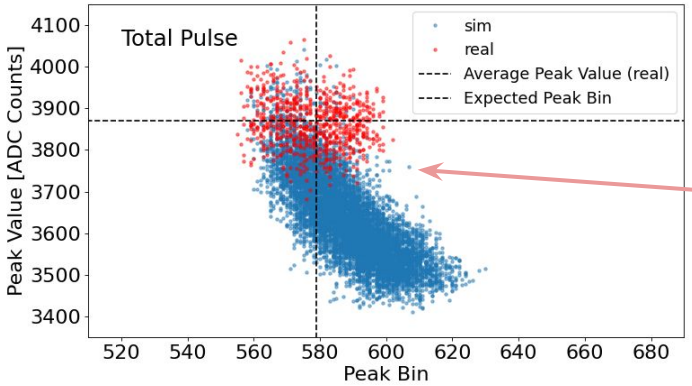

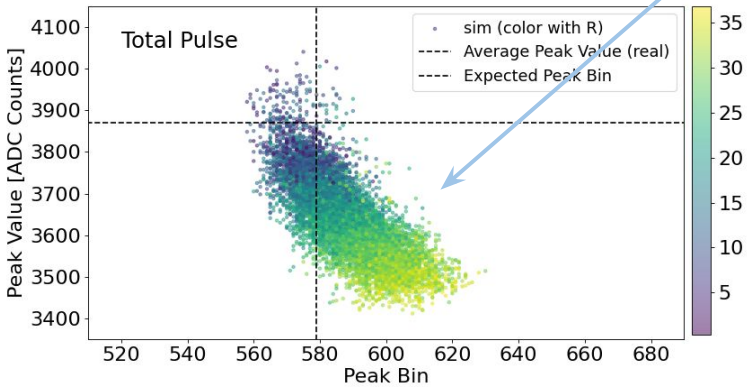

The simple expectation is that the total pulse does not vary much as a function of interaction positions

- ‘real’ appears to have no correlation, consistent with the expectation
- ‘sim’ has clear correlation with interaction position
  - When R is larger, ***Peak Bin*** gets later and ***Peak Value*** smaller
  - ‘sim’ differ more from ‘real’ when R gets larger

Not obvious why this happens in the simulation so we show additional clues on the next pages

Comparison, Outer and Inner Pulse, Val542

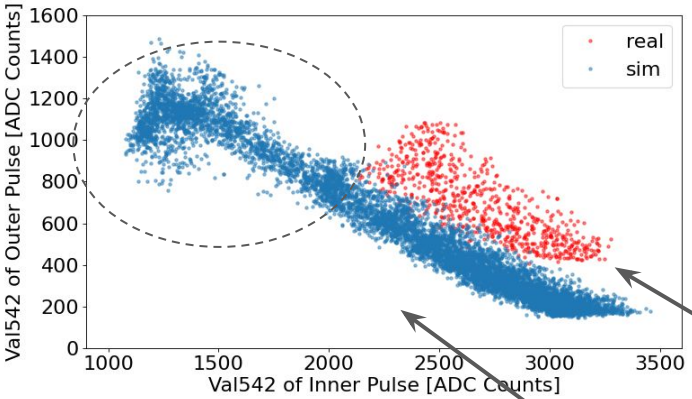

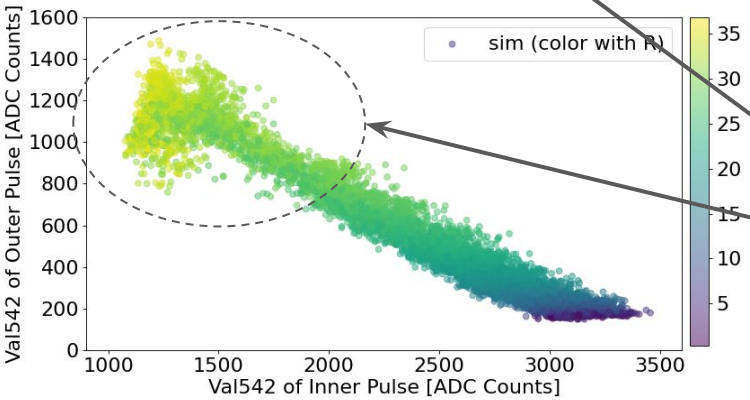

Qualitatively we expect there to be a simple R-dependent relationship between the Fast Energy sharing in the outer channel (PA) and the combined inner channels (PB+PC+PD):

less Fast Energy in the inner channels while more Fast Energy in the outer channel

- Both ‘sim’ and ‘real’ exhibit a similar trend, qualitatively consistent with the expectation
  - ***Val542***(inner) is smaller while ***Val542***(outer) is larger
- The ‘real’ distribution is clearly above ‘sim’
- The events with larger R in ‘sim’ don’t have a counterpart in ‘real’ (dashed circle) ?

Comparison, Individual Pulses (PA/PB/PC/PD), Peak Value vs Peak Bin

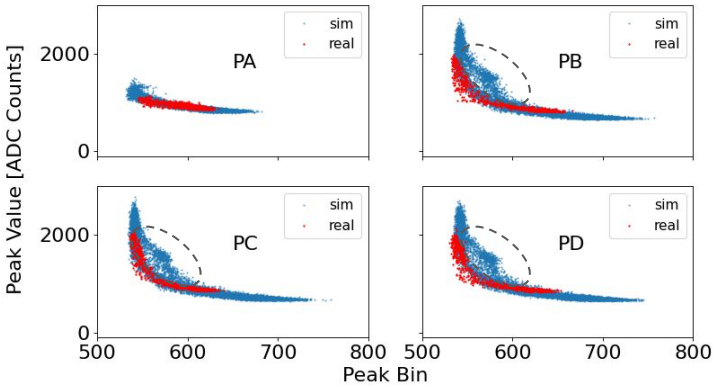

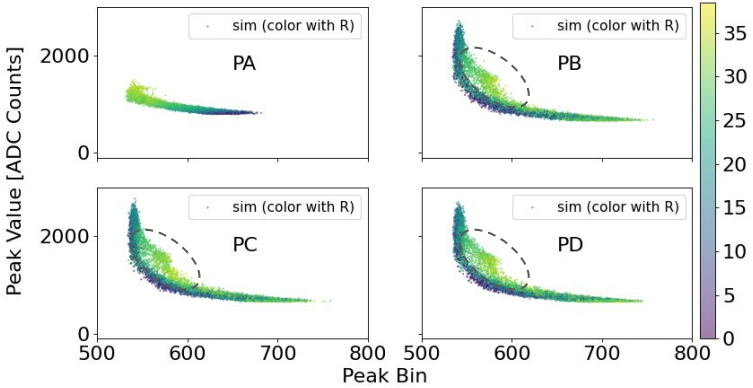

Moving to individual channels, we expect the quantity value to have larger variation due to both R and |ΔΦ| dependence. Also, as PA and PB/PC/PD have difference shape, we expect similarity between inner channels channels but differences for the outer channel.

- Both ‘sim’ (for R < 25 mm) and ‘real’ are qualitatively consistent with our expectations
  - PB, PC, PD have the same L-Shape distribution
  - PA has a linear-like shape distribution
- But ‘Sim’ has an extra group of events outside the L-Shape for PB/PC/PD with large R (>25mm, dashed circle)

Comparison, Individual Pulses (lead/near/away), Peak Value vs Peak Bin

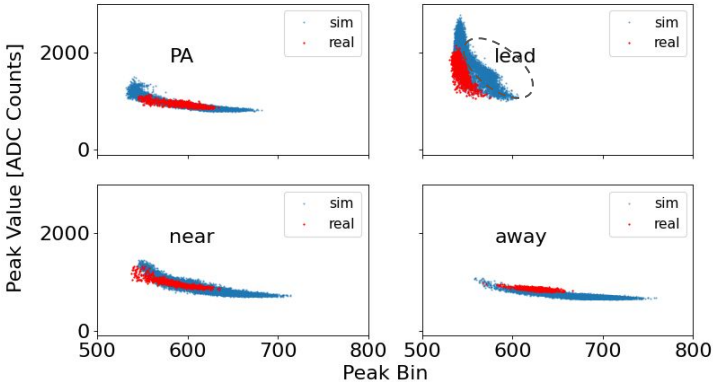

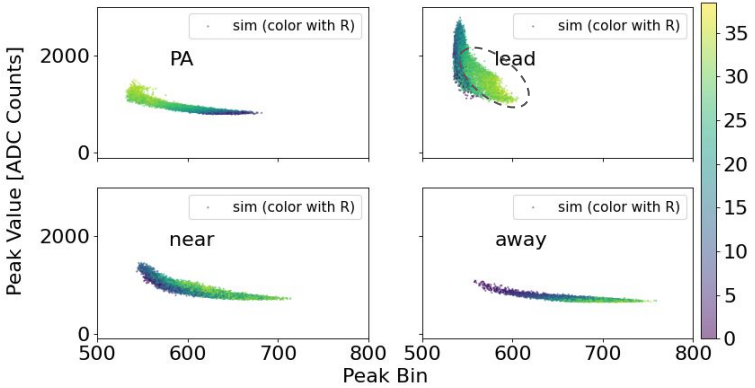

The lead/near/away collects different amounts of Fast Energy, the value distributions are expected to be different: The L-shaped distribution splits into three parts for both sim' and 'real'.

- The extra group of events away from the L-Shape in sim' is from the **lead channel** (dashed circle)

This does not tell us the cause of the differences, but suggests that it has something to do with the fast phonons which are the hardest to model correctly

Recap: Summary of Similarities and Differences

- The distributions of all three early-portion quantities appear to be consistent with the Fast/Slow Energy modeling
  - When collecting more Fast Energy, a channel or combined channels has a larger ***Val542***, an earlier ***Peak Bin***, and a larger ***Peak Value***
  - For total pulse, the variations of these quantities in real data is uncorrelated, while those in simulated data is correlated
- The distributions of these quantities have similar shapes between simulation and real data, but are quantitatively quite different
  - The distributions are wider in simulation than real data.
  - The mean value of these quantities are different
  - Simulation shows these quantities are correlated to R and are most visibly different for R>25mm
  - Unfortunately, we don't have a reliable estimate of R the real data (our hope had been that the simulation was going to tell us how to get it right)

Preliminary Hypotheses to Potentially Explain the Differences

Since the resolution of the differences will need to be left for later analysis, we identify several preliminary hypotheses that could potentially explain the differences observed in the comparison of the pulse shape quantities between the simulation and real data.

1. The parent distribution for simulated and real data are different
    - Selection bias: If events have smaller peak values than expected, they might not be in our real data due to our selection methods, and thus excluded from the sample for comparison
    - Production bias: The Ge-71 decay events in the Ge crystal might not be uniformly distributed as is assumed in simulation
2. Timing differences between simulated and real pulses

Plot: the example simulated total pulse begins to rise at 10 bins (16 μs) later than the Average Template

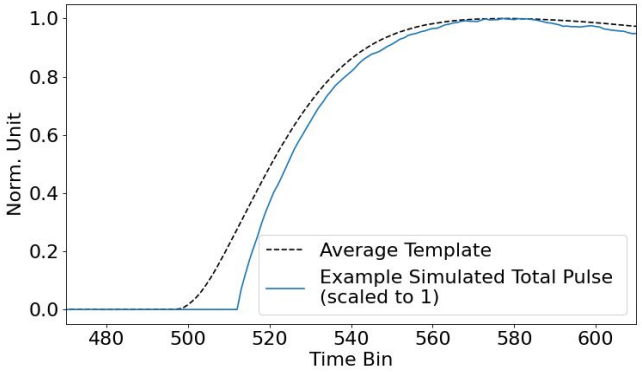

Preliminary Hypotheses to Potentially Explain the Differences (cont.)

Since the resolution of the differences will need to be left for later analysis, we identify several preliminary hypotheses that could potentially explain the differences observed in the comparison of the pulse shape quantities between the simulation and real data.

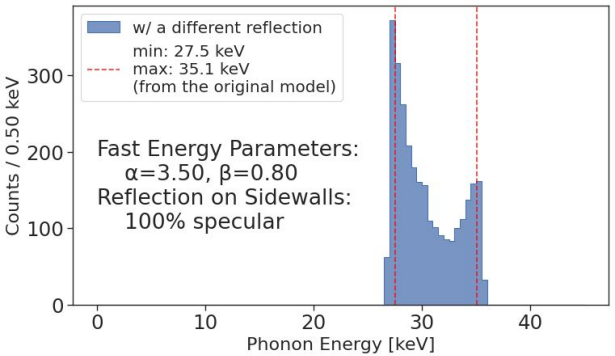

3. Phonon Reflection mismodeled in simulation
   - The current simulation models **100% diffuse reflection** (a phonon reflects into a random direction).
   - There might be a portion of **specular reflection** on the polished surfaces of the detector (a phonon reflects like light reflects on a mirror)
     (Plot: 100% specular reflection on the sidewall using a simple model)
4. Charge Transport mismodeled in simulation
   The current model implementation in simulation may not fully or accurately represent the physical processes, and thus could affect the distributions of energies and emission positions of the phonons

Outline

- **Introduction**
  - Evidence for Dark Matter and the WIMP Hypothesis
  - Overview of the SuperCDMS Soudan Experiment and the CDMSlite Detector
  - Thesis Goals
- **CDMSlite Detector Physics**
  - Electron Recoil Interactions
  - Detector's Response and Output
- **CDMSlite Experimental Data for this work**
- **SuperCDMS Simulation and CDMSlite Simulation Samples**
- **Data Analysis**
  - Collection Efficiency
  - Energy Collection over Position and Time
  - Simulation-based Analysis Methods using Pulse Shape Characteristics (Rejecting Poorly-Measured Events, Estimating Interaction Positions, Calibrating Real Pulses)
  - Comparison of Pulse Shapes between Simulated and Real Experiment Data
- **Future Work and Conclusions**

Future Work

Based on the hypotheses we proposed to potentially explain the existing differences observed from the comparisons, we comment on some of the concrete steps for the long-term SuperCDMS simulations efforts to move forward, some of which have been solved or are in progress by the next generation of students:

- Correct the different timing offsets between simulation and real pulses (Done, by Rik Bhattachryya)
- Update the charge transport and scattering models in the simulation (Done, Iman Ataee Langroudy)
- Improve the understanding of the physical processes that govern the phonon energy and mode evolution at each stage of the pulse (In progress, by Rik Bhattachryya)
- Incorporate specular phonon reflections in the simulation and surface effects such as surface-mediated downconversion (In progress, Nolan Tenpas)
- Re-tune relevant simulation parameters and identify missing/broken modeling (In progress, Dylan Monteiro)

Conclusions

- We have compared our advanced simulations of 10 keV electron recoil events in the CDMSlite detector to the corresponding photon/electron events from Ge-71 decay in real CDMSlite data to deepen our understanding of its response for use in dark matter searches.
- The simulations suggest that some assumptions in previous analyses are well-justified (fast and slow energy model), while others are not (identical tails in all channels).
- We have advanced our understanding of Fast Energy with a more sophisticated generalized Gaussian model, and developed new analysis methods using pulse shape quantities that should be useful in the future assuming our simulation can achieve high fidelity
- Our simulation qualitatively matches expectations, but shows quantitative differences from real pulses, suggesting future work on modeling refinement of in simulation and analysis is needed.
- We expect that this work will be used in analyzing the data from the upcoming datataking runs at SNOLAB in the next couple of years, and hopefully enable a discovery of dark matter.

BackUp Pages

Previous CDMSlite Analysis: Energy Quantity Constructed from Pulses

- Assumption: A pulse is produced by the phonon sensors when an interaction occurs inside the detector. The amplitude of summed pulse from the all four phonon channels is proportional to the total energy generated inside the detector
- Methods: using the Optimal Filter (OF) algorithms that take in the expected pulse shape (i.e. pulse template) and an expected noise (power spectrum distribution, PSD) to fit a real, noisy pulse, and determine the amplitudes

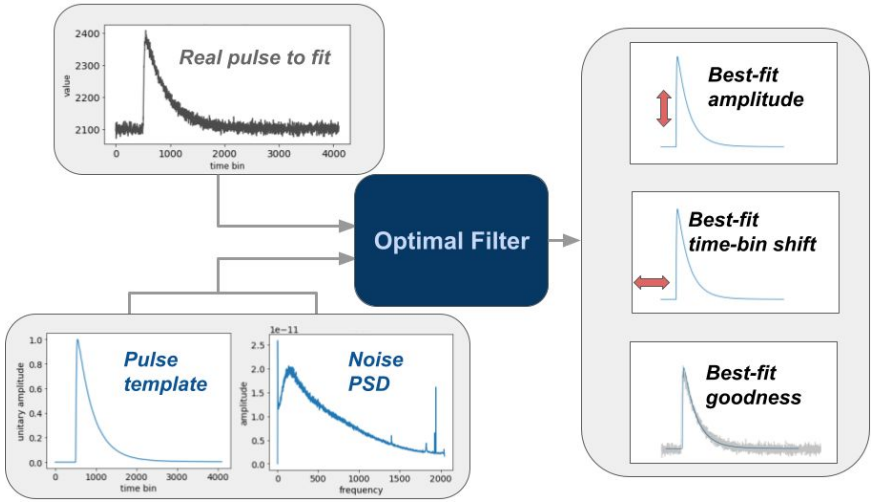

One-Template OF with Non-Stationary Noise

- Average Template
  The averaged shape of the pulses in the real data
- Non-Stationary Noise
  A noise PSD that varies with time, including the extra variation introduced by the pulse.

This OF algorithm gives us the best-fit amplitude (PTNFamps) estimate the total energy in the previous CDMSlite analysis. In this work we use PTNFamps as the energy quantity for use in event selection.

Overview of CDMSlite Detector's Response and Signal Readout

(Note: here we overview the CDMSlite detector's response to an interaction, with more details to be described in later pages.)

When an interaction occurs insides the CDMSlite detector,

① The deposited energy produces charges (such as electrons)

② Charges travel toward the detector surface, as pulled by electric field, and collide with germanium lattices to produce lattice vibrations (phonons)

③ Phonons could be absorbed by the phonon sensors at early time, or experience scattering and reflection before absorption

④ Phonon sensors generate (downward) signals when absorbing phonons

⑤ A pulse (upward) is recorded after a signal is processed by readout electronics

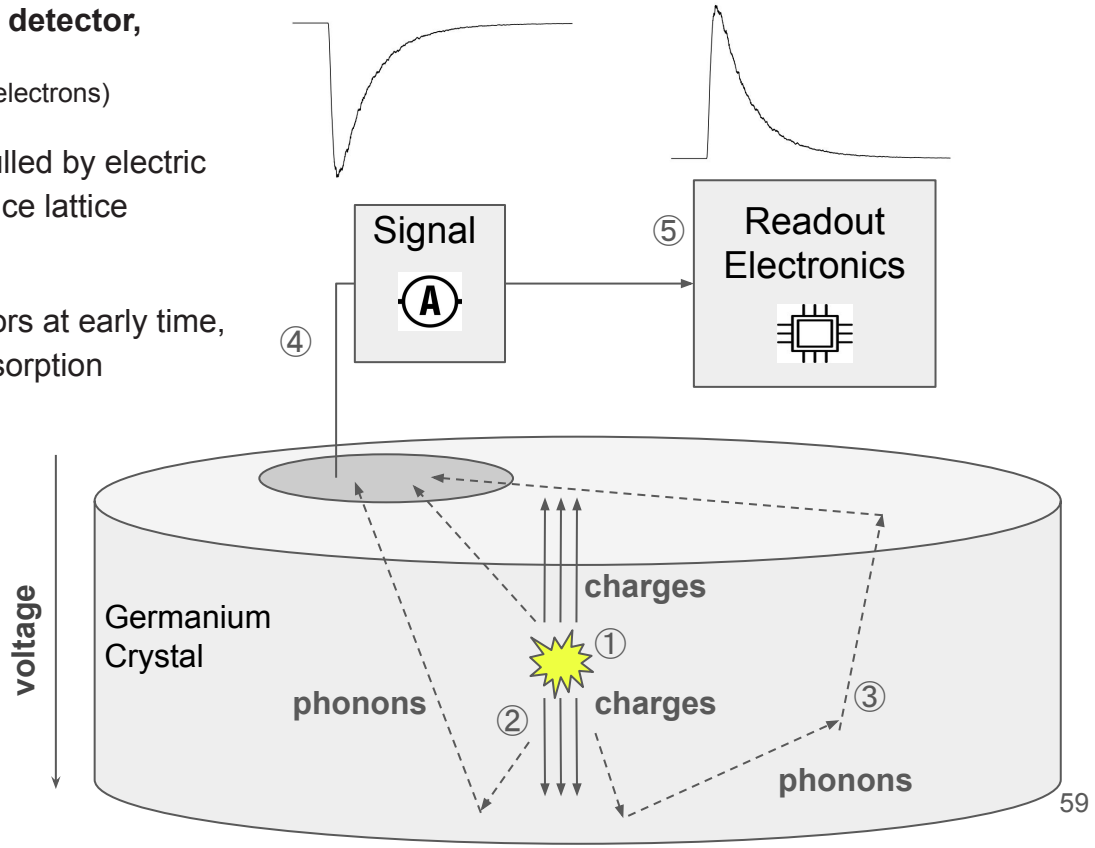

Compare Pulse Shape to Expectations, Total Pulse

Here we compare a simulated total pulse (randomly selected in the EPot sample) to the expected shape (Average Template)

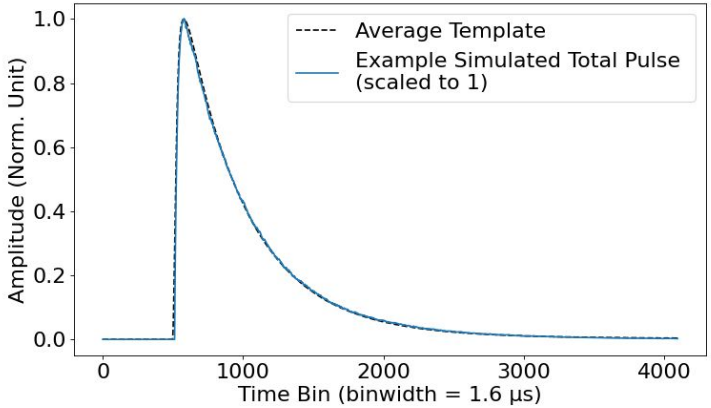

The simulated total pulse visually has excellent overlap with the Average Template, but with noticeable deviations at the early portion and the far end.

(Due to the absence of noise in the samples used in this work, the pre-pulse region (Bin < ~ 500, or time <~ 800 μs) of the simulated pulse is zero.)

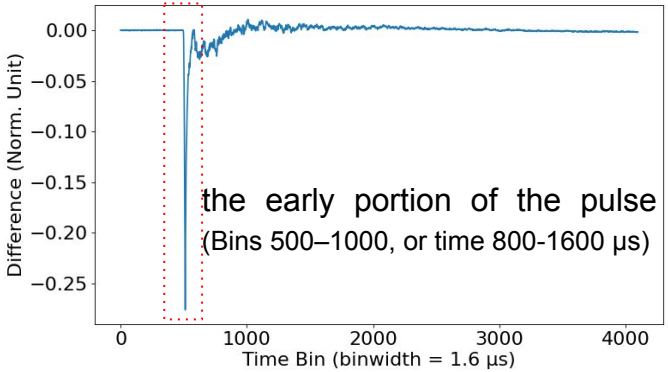

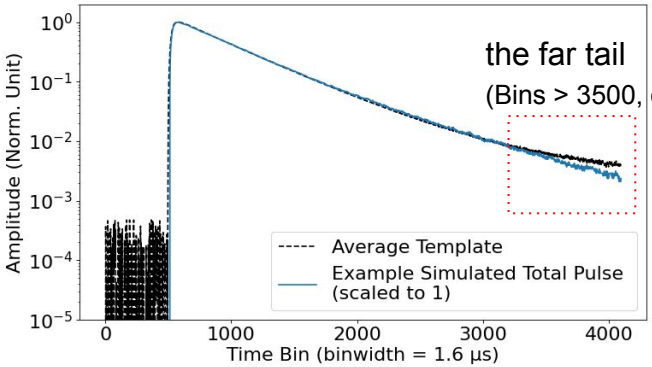

Ge-71 Electron Capture Decay

Ge-70 + n -> Ge-71

Ge-71 + e -> Ga-71

Ga-71 emits photons and electrons and releases its atomic binding energy

- Lower orbit, higher possibility, more energy released
- Consider orbits highlighted with red rectangle

31–Ga	K	2.00	10331.0	13222.0	25.6450	8.63840– 1	8.31930– 1	4649.27	5582.21	99.5174
	L1	2.00	1290.70	2577.90	114.420	6.64890– 3	8.69970+ 0	12.7845	1185.73	92.1847
	L2	2.00	1150.40	2568.50	98.7020	9.11830– 3	7.46030– 1	13.4359	1074.63	62.3345
	L3	4.00	1122.00	2462.50	100.560	8.93490– 3	7.52560– 1	12.3619	1043.22	66.4171
	M1	2.00	157.750	582.900	341.060	3.69570– 5	4.45700+ 0	0.00517	99.2220	58.5229
	M2	2.00	111.010	532.720	349.590	1.28640– 4	3.92590+ 0	0.00408	71.1520	39.8540
	M3	4.00	107.280	512.190	355.030	1.18000– 4	3.71490+ 0	0.00341	61.7004	45.5762
	M4	4.00	27.3700	382.070	403.920	7.64460– 8	1.29660– 2	0.00000	11.7009	15.6691
	M5	6.00	26.8700	377.320	406.630					26.8700
	N1	2.00	11.6900	59.7300	1192.10					11.6900
	N2	0.33	5.00000	27.4800	1774.00					5.00000
	N3	0.67	4.88000	25.9100	1816.10					4.88000

2-3, Part 2 EADL Atomic Subshell Parameters, Evaluated Atomic Data Library (EADL)

Phonon Decay, Scattering and Reflection before being Absorbed by QET

After the initial generation, phonon transport within the Ge crystal, undergoing decay, scattering and reflection processes before absorption by the sensors

- Decay
  - High-energy phonons (frequency > 1 THz or energy > 4 meV) decay instantly into lower-energy phonons.
  - Lower-energy (sub-THz) phonons can decay in a few μs and undergoing multiple random scatterings within a few mm
- Scattering
  - Lower-energy (sub-THz) phonons scatter at a randomized angle when they encounter different Ge atoms (e.g. Ge-70 to Ge-72). The average distance between two scatters is comparable to the detector size (~cm).
- Reflection
  - When a phonon reaches a QET unit, it is either absorbed with a finite probability, or reflected back into the Ge crystal.
  - When a phonon reaches the detector sidewall or any uncovered region of the detector surfaces, it is reflected.

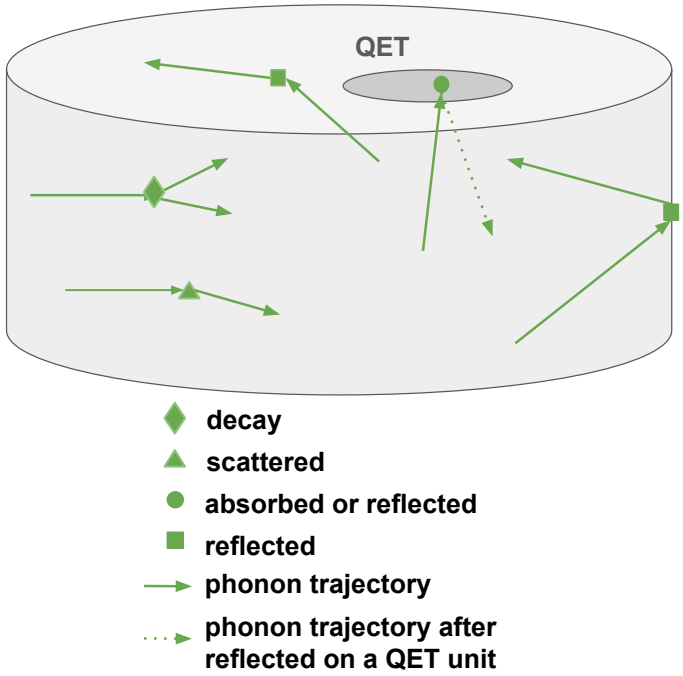

Separating Well- and Poorly-Measured Events

We visualize the distributions of **$\text{PeakBin}_{\text{lead}}$** and **$\text{Val542}_{\text{A}}/\text{Val542}_{\text{BCD}}$** for both well- and poorly-measured events, and establish criteria to separate them

$\text{PeakBin}_{\text{lead}}$

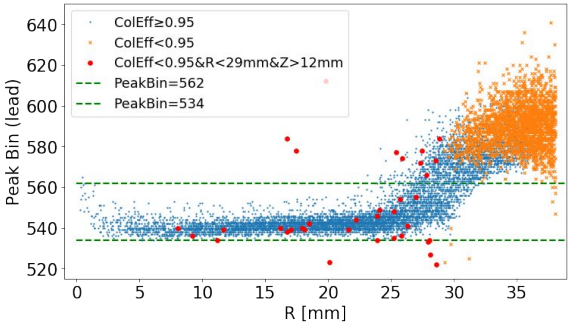

Val542_{A} / $\text{Val542}_{\text{BCD}}$

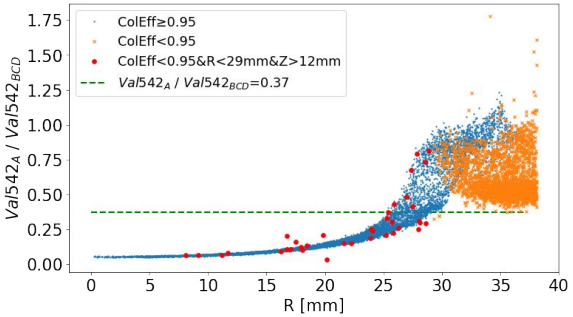

Val542_{A} / $\text{Val542}_{\text{BCD}}$ & $\text{PeakBin}_{\text{lead}}$

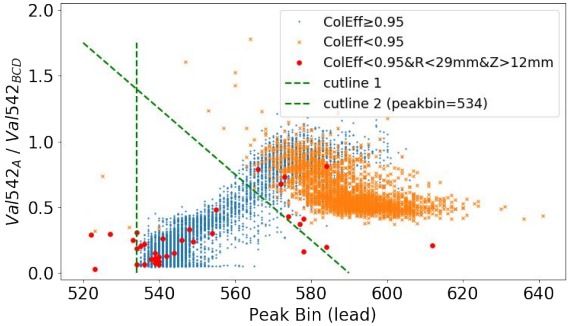

Selection Criteria and Number of Accepted and Rejected Events

Selection Criteria	Pass or Fail	Well-Measured (ColEff $\geq$ 0.95) 7860 events	Poorly-Measured (ColEff < 0.95) 2140 events
$534 \leq PeakBin_{lead} \leq 562$	Pass	5925 (75.4%)	
	Fail		2115 (98.8%)
$Val542_A/Val542_{BCD} \leq 0.37$	Pass	5306 (67.5%)	
	Fail		2109 (98.5%)
$(PeakBin_{lead} \geq 534)$ & $(Val542_A/Val542_{BCD}$ $+0.025 \times PeakBin_{lead} \leq 14.75)$	Pass	6112 (77.8%)	
	Fail		2119 (99.0%)

- All three methods are able to reject >98% of the poorly-measured events while keeping ~70% of well-measured events.
- Best results: the joint criterion rejects 99% of the poorly-measured events and retains 78% of the well-measured events

Statistical Results, Tails of Simulated Pulses

Value@2ms [ADC Counts]

Channel	$\mu_{Value@2ms}$	$\sigma_{Value@2ms}$	$\sigma_{Value@2ms}/\mu_{Value@2ms}$
PA	244.46±0.05	5.75±0.05	2.35%
PB	234.30±0.07	5.65±0.07	2.41%
PC	234.33±0.09	5.49±0.09	2.34%
PD	234.45±0.05	5.58±0.05	2.38%

Amplitude [ADC Counts]

Channel	$\mu_{Amplitude}$	$\sigma_{Amplitude}$	$\sigma_{Amplitude}/\mu_{Amplitude}$
PA	238.56±0.03	3.07±0.03	1.29%
PB	228.66±0.04	2.97±0.04	1.30%
PC	228.57±0.03	2.94±0.04	1.29%
PD	228.65±0.03	2.89±0.03	1.27%

Fall Time [ms]

Channel	$\mu_{FallTime}$	$\sigma_{FallTime}$	$\sigma_{FallTime}/\mu_{FallTime}$
PA	0.8441±0.0001	0.0087±0.0001	1.03%
PB	0.8343±0.0001	0.0088±0.0001	1.05%
PC	0.8347±0.0001	0.0090±0.0001	1.07%
PD	0.8344±0.0001	0.0089±0.0001	1.07%

Integral Area [ADC Counts · ms]

Channel	$\mu_{IntegralArea}$	$\sigma_{IntegralArea}$	$\sigma_{IntegralArea}/\mu_{IntegralArea}$
PA	201.36±0.02	1.89±0.02	0.94%
PB	190.78±0.02	1.78±0.02	0.93%
PC	190.80±0.02	1.80±0.02	0.95%
PD	190.78±0.03	1.81±0.03	0.95%

- PB, PC, PD have the same results within uncertainties
- PA has a bit larger values for all four quantities, for reasons we don't know yet
- All ***Fall Times*** are larger than expected value (0.823 ms)
- ***Tail Amplitude*** is a bit smaller than ***Value@2ms*** as the fitting range is the whole tail whose later time has a different ***Fall Time*** from earlier time

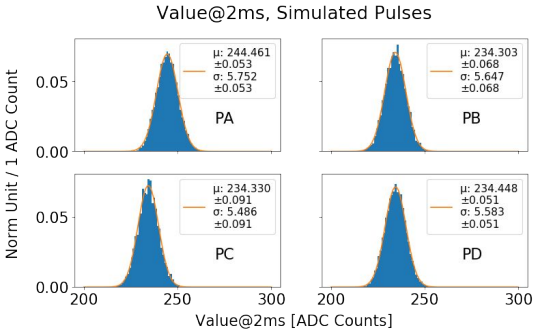

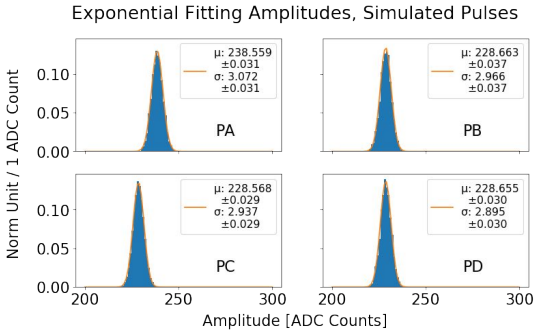

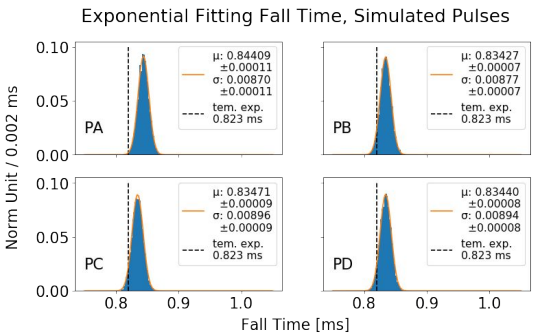

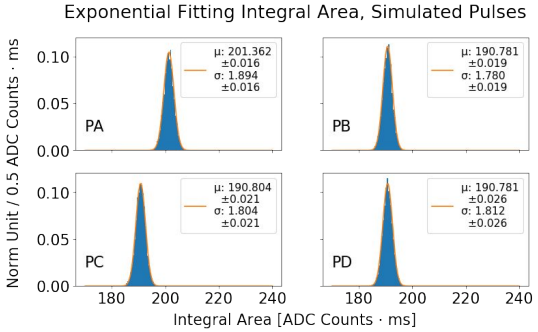

Statistical Results, Tails of Real Pulses

Value@2ms [ADC Counts]

Channel	$\mu_{Value@2ms}$	$\sigma_{Value@2ms}$	$\sigma_{Value@2ms}/\mu_{Value@2ms}$
PA	346.4±0.3	9.15±0.3	2.64%
PB	331.5±0.4	9.84±0.4	2.97%
PC	356.9±0.5	10.29±0.5	2.88%
PD	286.4±0.3	9.85±0.3	3.44%

Amplitude [ADC Counts]

Channel	$\mu_{Amplitude}$	$\sigma_{Amplitude}$	$\sigma_{Amplitude}/\mu_{Amplitude}$
PA	336.4±0.2	6.0±0.3	1.77%
PB	324.7±0.2	5.4±0.2	1.65%
PC	348.3±0.2	5.9±0.2	1.70%
PD	279.9±0.2	5.6±0.2	2.00%

Fall Time [ms]

Channel	$\mu_{FallTime}$	$\sigma_{FallTime}$	$\sigma_{FallTime}/\mu_{FallTime}$
PA	0.845±0.003	0.0484±0.003	5.73%
PB	0.807±0.001	0.0268±0.001	3.32%
PC	0.820±0.001	0.0284±0.001	3.46%
PD	0.815±0.002	0.0419±0.002	5.14%

Integral Area [ADC Counts · ms]

Channel	$\mu_{IntegralArea}$	$\sigma_{IntegralArea}$	$\sigma_{IntegralArea}/\mu_{IntegralArea}$
PA	285.2±0.5	13.9±0.5	4.86%
PB	262.8±0.2	8.3±0.2	3.17%
PC	286.4±0.4	10.1±0.4	3.52%
PD	228.4±0.6	11.0±0.6	4.80%

- All the measurement resolutions (σ/μ) are larger than simulation due to noise
- All four quantities are statistically different between channels
- All ***Fall Times*** appear to be consistent with the expected value (0.823 ms)
- PA and PD have larger resolutions in ***Fall Time*** and ***Integral Area*** than PB and PC, indicating PA and PD might be more noisy

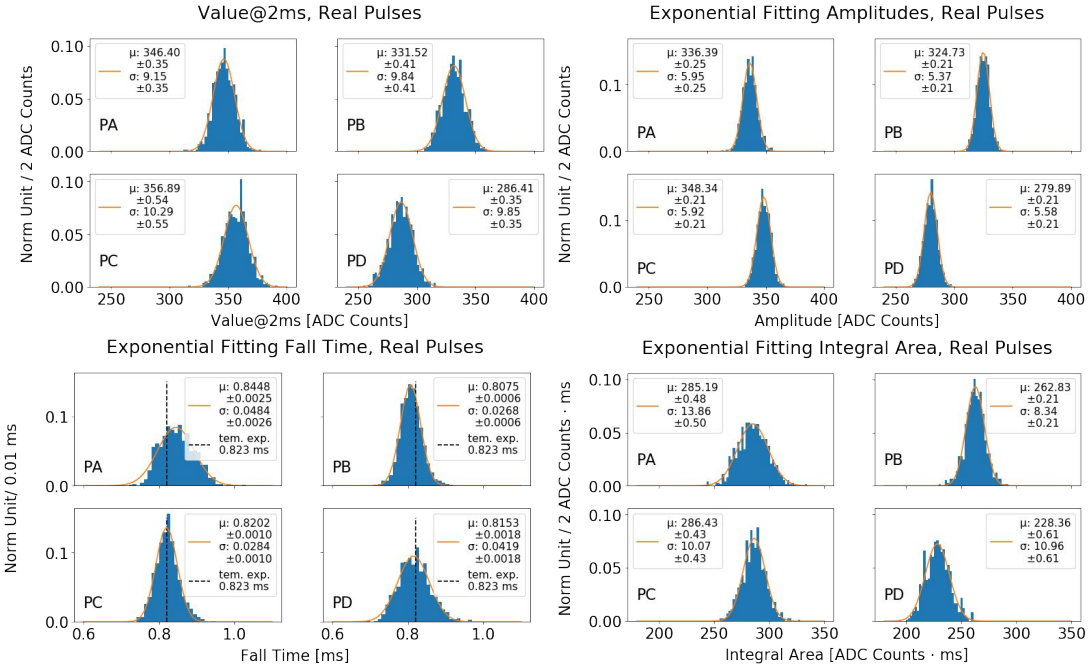

Comparison of Pulse Tail Quantities after Relative Calibration

Let's compare the four pulse tail quantities of real pulses after relative calibration (real) to those of simulated pulses (sim)

- All channels match
- Real has wider distributions due to noise in real world
- The average of ***Value@2ms*** of sim is larger the real
- The average of ***Fall Time*** of real are larger than sim

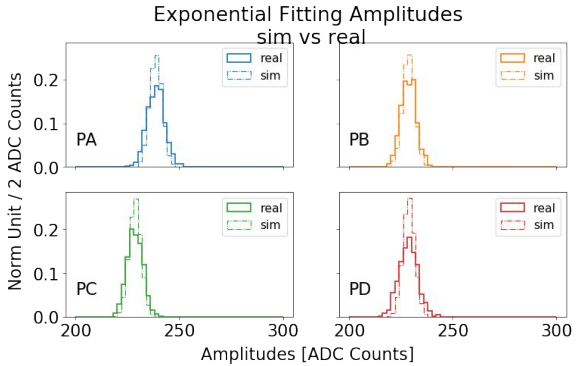

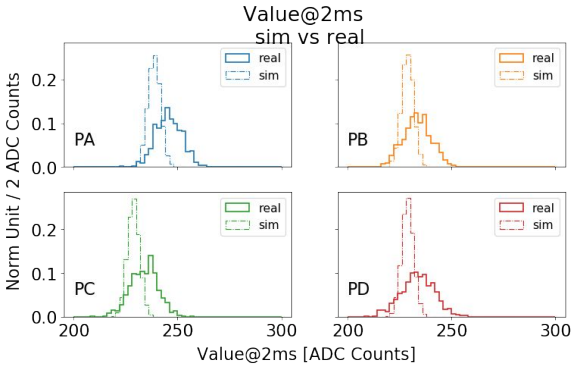

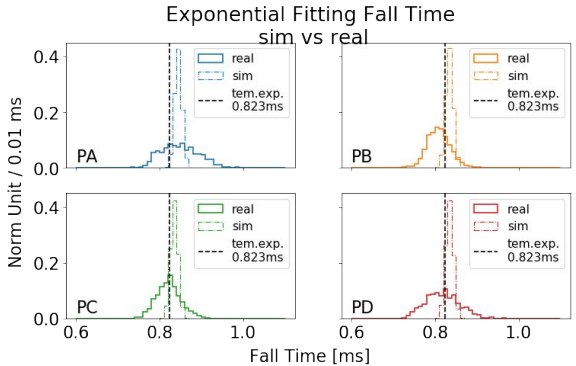

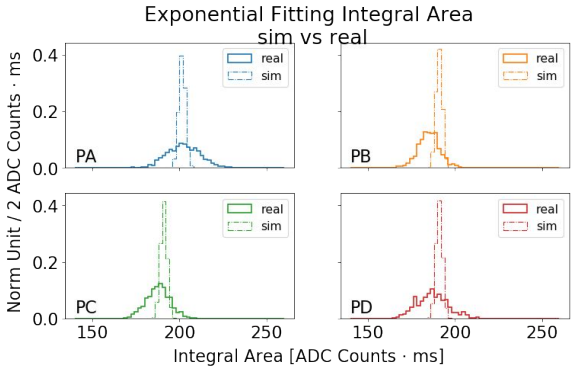

Choosing *Tail Amplitude* to Calibrate the Real Pulses

- We choose ***Tail Amplitude*** to calculate the constants for the channel-by-channel relative calibration on real pulses.
  - ***Tail Amplitude*** exhibits the smallest overall measurement resolutions (the fractional standard variation, σ/μ) *
- Constants Calculation
  We dividing the mean (μ) of ***Tail Amplitude*** of the simulated pulses by that of the real pules.
  PA: 0.709; PB: 0.704; PC: 0.656, PD: 0.817
- Calibrating Real Pulses
  We multiply the pulse values by its corresponding calibration constant.
  - real PA pulse * 0.709
  - real PB pulse * 0.704
  - real PC pulse * 0.656
  - real PD pulse * 0.817

Comparison of Measurement Fractional Standard Variations (σ/μ) for Pulse Tail Quantities

Channel	*Value@2ms*		*Amplitude*		*Fall Time*		*Integral Area*	
	real	sim	real	sim	real	sim	real	sim
PA	2.64%	2.35%	1.77%	1.29%	5.73%	1.03%	4.86%	0.94%
PB	2.97%	2.41%	1.65%	1.30%	3.32%	1.05%	3.17%	0.93%
PC	2.88%	2.34%	1.70%	1.29%	3.46%	1.07%	3.52%	0.95%
PD	3.44%	2.38%	2.00%	1.27%	5.14%	1.07%	4.80%	0.95%

Comparison of Measurement Mean (μ) for Pulse Tail Quantities

Channel	*Value@2ms*		*Amplitude*		*Fall Time*		*Integral Area*	
	real	sim	real	sim	real	sim	real	sim
PA	346.37	244.46	336.39	238.56	0.8448	0.8441	285.19	201.36
PB	331.51	234.30	324.73	228.66	0.8075	0.8343	262.83	190.78
PC	356.94	234.33	348.34	228.57	0.8202	0.8347	286.43	190.80
PD	286.31	234.45	279.89	228.65	0.8153	0.8344	228.36	190.78

Calibration Constants based on *Amplitude*

Channel	Constant	Calculated by
PA	0.709	238.56/336.39
PB	0.704	228.66/324.73
PC	0.656	228.57/348.34
PD	0.817	228.65/279.89

* While the smallest variation for any distribution is ***Integral Area*** for simulation, ***Tail Amplitude*** exhibits variations below 2% in both simulated and real data, making it the lowest overall variation.

Comparison, Total Pulse, Overview of Each Quantity Distribution

‘sim’

- ***Val542*** has not Gaussian-like distribution
- ***Peak Bin*** looks fairly Gaussian distribution but is shifted to earlier times than for ‘real’
- ***Peak Value*** has not Gaussian-like distribution

’real’ (results are consistent with expectation)

- ***Val542*** has Gaussian-like distribution
- ***Peak Bin*** has Gaussian-like distribution around 579 as expected
- ***Peak Value*** has Gaussian-like distribution

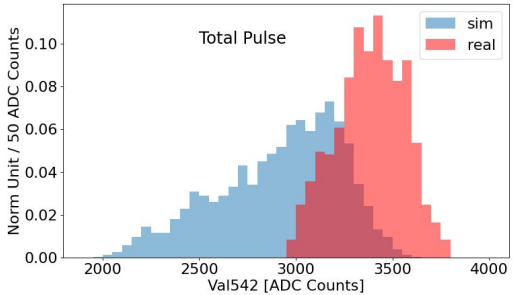

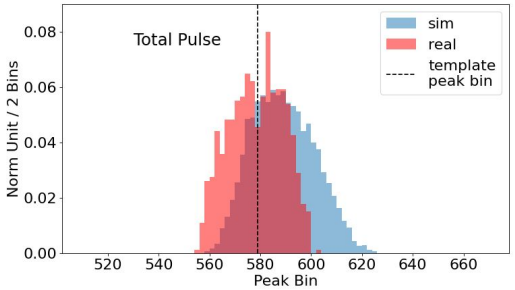

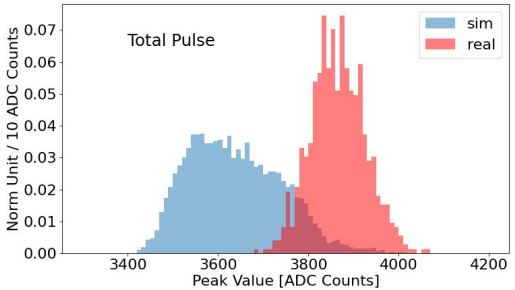

Comparison, Outer and Inner Pulse, Overview of Each Quantity Distribution

- Each distribution in both ‘sim’ and ‘real’ is wider compared to that for total pulse due to R dependence
- Each distribution in ‘sim’ has much bigger variation than ‘real’, with overlapping portions
- Each distribution in ‘sim’ have two-bump shape, while that in ‘real’ is single-bump shape

Inner Pulse

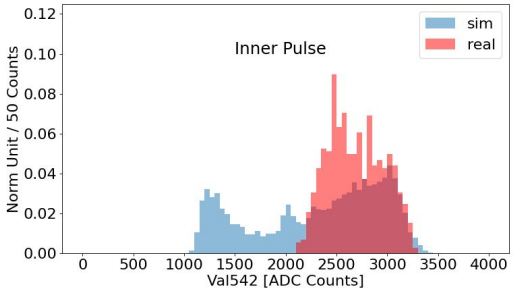

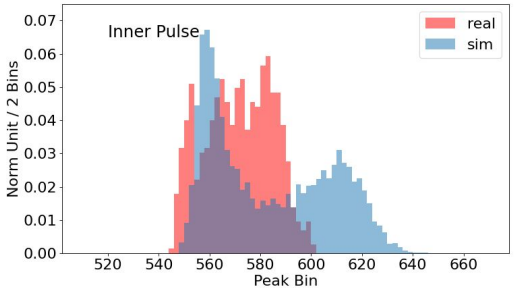

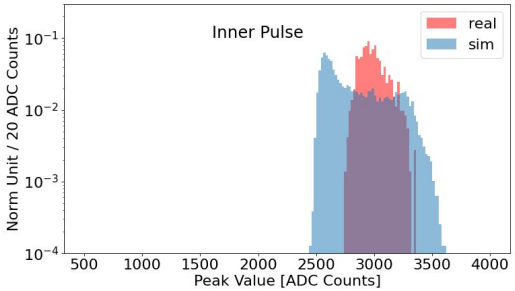

Outer Pulse

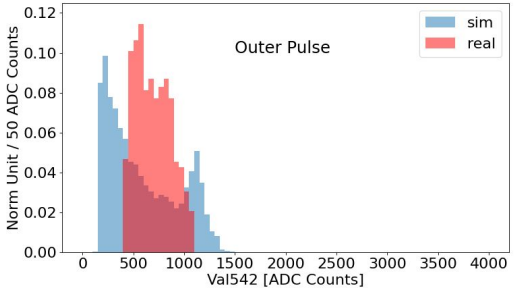

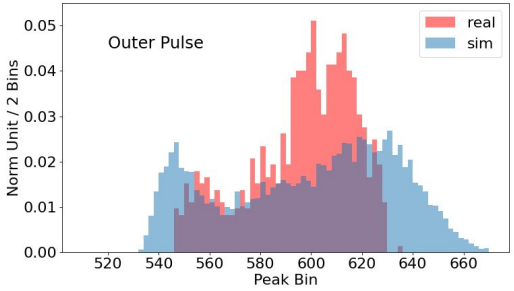

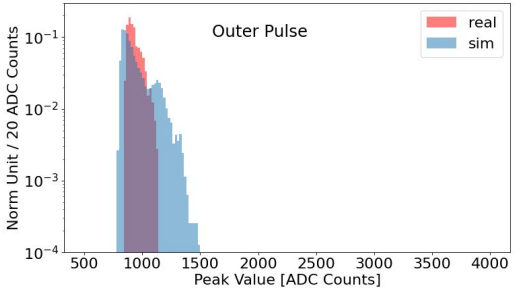

Comparison, Outer and Inner Pulse, Peak Value vs Peak Bin

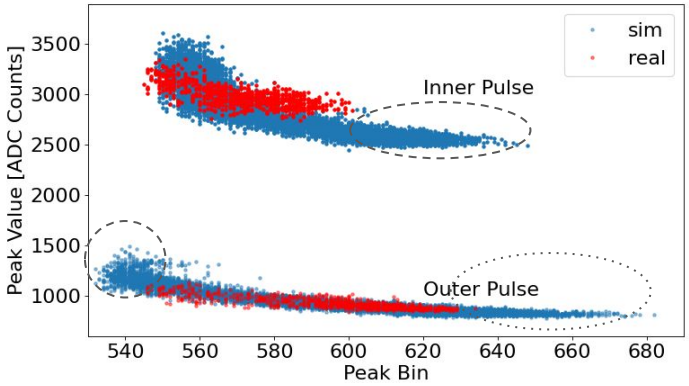

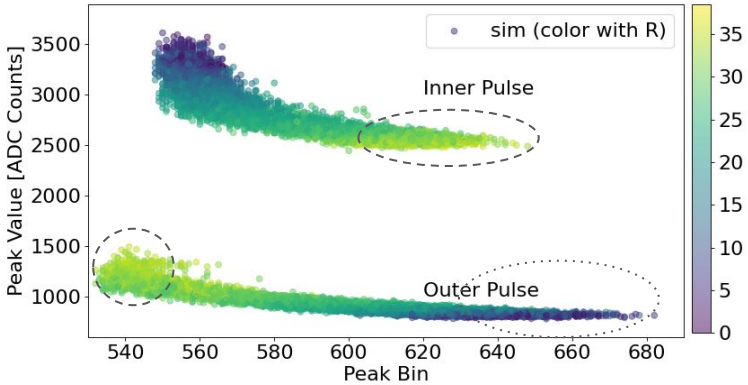

‘sim’ vs. ‘real’

- Both ‘sim’ and ‘real’ have overlapping distributions and exhibit a similar trend
  (***Peak Value*** decreases as a function of ***Peak Bin***)
- The ‘sim’ distribution is wider than the ‘real’

In ‘sim’

- The correlation between ***Peak Value*** and ***Peak Bin*** varies significantly with R for both the outer and inner pulses
- There are differences at both large R (>25mm, dashed circle) and small R (<10 mm, dotted circle)

Comparison, Individual Pulses (PA/PB/PC/PD), Overview of Each Quantity Distribution

(Note: color code is changed here. ‘sim’:dashed; ‘real’: solid; PA/PB/PC/PD: blue/orange/green/red)

- Similarities: For both ‘sim’ and ‘real’, PB, PC and PD have the same distribution shape, but PA has a different one, as expected
- Differences: All ‘sim’ distributions are wider than ‘real’

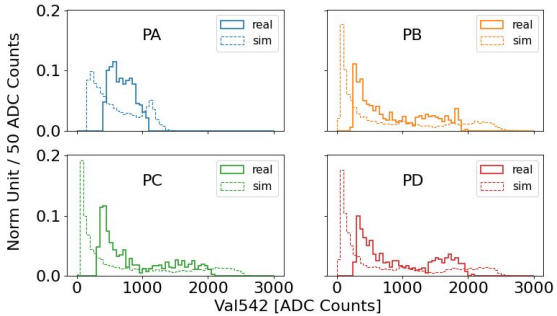

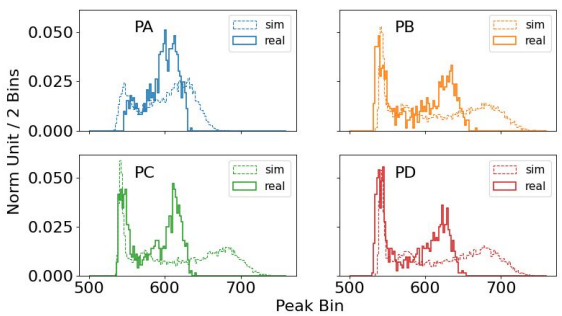

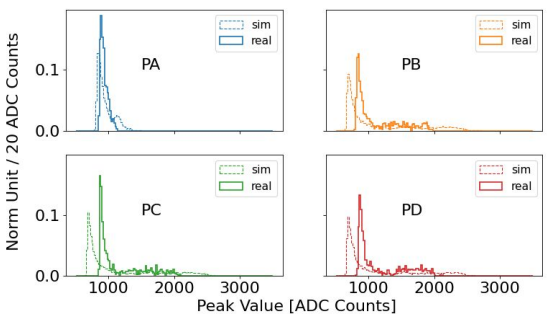

Comparison, Individual Pulses (lead/near/away), Overview of Each Quantity Distribution

(Note: color code is changed here. ‘Sim’: dashed; ‘real’: solid; PA/lead/near/away: blue/orange/green/red)

- Similarities: For both ‘sim’ and ‘real’, the **lead/near/away pulses** have **largest/larger/smallest** *Val542*, **earliest/earlier/later** *Peak Bin* and **largest/larger/smaller** *Peak Value*, as expected
- Differences: All ‘sim’ distributions are wider than ‘real’. The *Peak Bin* of the lead pulse in ‘sim’ has a two-bump shape while that in ‘real’ has a single-bump shape.